Appendix A12

Geotechnical Analyses of Proposed Laboratory Excavations at the Former Homestake Mine Lead, South Dakota, Golder Associates 06-1117-014 (May 2006)

Golder Associates Ltd.

2390 Argentia Road
Mississauga, Ontario, Canada L5N 5Z7
Telephone: (905) 567-4444
Fax: (905) 567-6561

FINAL
REPORT ON

GEOTECHNICAL ANALYSES OF PROPOSED LABORATORY EXCAVATIONS AT THE FORMER HOMESTAKE MINE LEAD, SOUTH DAKOTA

Submitted to:

Lawrence Berkeley National Laboratory
One Cyclotron Road
Berkeley, California
94720

DISTRIBUTION:

2 Copies - Lawrence Berkeley National Laboratory
2 Copies - Golder Associates Ltd.

May 2006 06-1117-014

TABLE OF CONTENTS

SECTION PAGE

TABLE OF CONTENTS I
1.0 INTRODUCTION 1
1.1 Scope of Work 1
2.0 EXISTING GEOTECHNICAL DATA 2
2.1 Intact Rock Properties 2
2.2 In situ Stresses 3
2.3 Rock Mass Ratings and Choice of Failure Criterion 4
2.3.1 Tunnelling Quality Index, Q' 4
2.3.2 Choice of Failure Criterion 5
3.0 NUMERICAL ANALYSES 8
4.0 NUMERICAL ANALYSES RESULTS 11
4.1 Spacing between Excavations 11
4.2 Orientation of Excavations 12
4.3 Depth of Excavations 13
4.4 Rockburst Potential 13
4.5 Ground Support 15
5.0 RECOMMENDATIONS 18
5.1 Excavations 18
5.2 Follow-up Geotechnical Investigations 19
REFERENCES 21

LIST OF TABLES

Table 1 Properties of Poorman Formation
Table 2 Analyses Naming Convention
Table 3 Preliminary Support Recommendations

LIST OF FIGURES

Figure 1 Homestake Dusel 4850L Lab Modules Concept
Figure 2 Poorman Formation w/ Chert – Hwy 14a No.2
Figure 3 Yates Unit Exposure in Blacktail Gulch, North of Central City, South Dakota
Figure 4 Close-up of Yates Unit Amphibolite in Blacktail Gulch
Figure 5 Excavation Sequence – 1st Room – Homestake
Figure 6 Excavation Sequence – Parallel Arrangement – All Rooms – Homestake
Figure 7 Excavation Sequence – 'En Echelon' Arrangement – All Rooms – Homestake

Figure 8 Location of Planes and Density of Results at Each Plane – Parallel Room Layout
Figure 9 Location of Planes and Density of Results at Each Plane – "En Echelon" Room Layout
Figure 10 Location of Voxel Box and Density of Results – Parallel Room Layout
Figure 11 Comparison of σ_1 Contours in MPa for Excavations at Variable Spacings
Figure 12 Vertical Stress Profile at Spring Line of Rooms – Parallel Room Layout
Figure 13 Effect of Orientation – Boundary Stresses (σ_1 - σ_3) – 8000L – Homestake
Figure 14 Effect of Orientation – Plastic Zone in Poorman Formation – 4850L – Homestake
Figure 15 Effect of Orientation – Plastic Zone in Poorman Formation – 7400L – Homestake
Figure 16 Effect of Orientation – Plastic Zone in Yates Unit – 7400L – Homestake
Figure 17 Effect of Orientation – Micro-cracking Extent in Yates Unit – 7400L – Homestake
Figure 18 Effect of Orientation – Plastic Zone in Yates Unit – 8000L – Homestake
Figure 19 Effect of Orientation – Micro-cracking Extent in Yates Unit – 8000L – Homestake
Figure 20 Effect of Stress (Depth) – Micro-cracking Extent in Yates Unit – Homestake
Figure 21 Effect of Stress (Depth) – Plastic Zone in Yates Unit – Homestake
Figure 22 Effect of Stress (Depth) – Plastic Zone in Poorman Formation – Homestake
Figure 23 Comparison of Stored Strain Energy, Plastic Zone and Micro-fracturing in Yates Unit – Homestake – 4850L
Figure 24 Comparison of Stored Strain Energy, Plastic Zone and Micro-fracturing in Yates Unit – Homestake – 8000L
Figure 25 Excavation Sequence – Plastic Zone in Poorman Formation – 4850L – Homestake
Figure 26 Excavation Sequence – Micro-cracking Extent in Poorman Formation – 4850L – Homestake
Figure 27 Excavation Sequence – Plastic Zone in Poorman Formation – 7400L – Homestake
Figure 28 Excavation Sequence – Micro-cracking Extent in Yates Unit – 4850L – Homestake
Figure 29 Excavation Sequence – Plastic Zone in Yates Unit – 8000L – Homestake
Figure 30 Excavation Sequence – Micro-cracking Extent in Yates Unit – 8000L – Homestake
Figure 31 Empirical Design of Support for Laboratory Roof – Poorman Formation
Figure 32 Empirical Design of Support for Laboratory Side Walls – Poorman Formation
Figure 33 Empirical Design of Support for Laboratory Roof – Yates Unit
Figure 34 Empirical Design of Support for Laboratory Side Walls – Yates Unit

LIST OF APPENDICES

Appendix A Initial Stability Study of Large Openings for the National Underground Science Laboratory at the Homestake Mine, Lead – Tesarick, D., Johnson, J., Zipf, Jr., K, and Lande., K., 2002

Appendix B Stope Stability as a Function of Depth at the Homestake Mine – Pariseau, W. and Duan, F.

Appendix C Destress blasting in hard rock mines – a state-of-the-art review – Mitri, H.S., and Saharan, M.R., 2006

1.0 INTRODUCTION

The former Homestake mine in Lead, South Dakota has been selected as a finalist by the National Science Foundation (NSF) to submit a proposal to develop this site for a Deep Underground Science and Engineering Laboratory (DUSEL).

Conversion of the mine to an underground lab includes excavation of various size openings at a number of locations within the mine. The proposal to NSF must demonstrate constructability of the required excavations necessary to house a variety of research experiments.

To this end, the Lawrence Berkeley National Laboratory has retained Golder Associates to conduct a preliminary geotechnical analysis of the proposed openings.

1.1 Scope of Work

The current development plans include lab excavations approximately 50 m long × 20 m wide × 15 m high. Room geometries and layouts have been provided in AutoCAD format by the Lawrence Berkeley National Laboratory (see Figure 1). These rooms are proposed to be excavated on the 4850L, 7400L and possibly the 8000L of the Homestake mine. The rooms would be developed primarily on the Yates Formation, and potentially on the Poorman Formation. The Lawrence Berkeley National Laboratory has asked Golder Associates to:

1. Investigate the potential zones of disturbances around the proposed excavations at 4850L, 7400L and 8000L within the Yates and Poorman formation.

2. Discuss the impact of the required opening sizes on construction techniques and the potential for rock bursting and other hazards or risks.

3. Make recommendations for optimal geometry and required ground support for short term and long term stability (design life for occupancy is 20 to 30 years).

4. Verify the proposed spacing between excavations to ensure that stress distributions created by new openings will have a minimum impact on the overall stability of neighbouring excavations (a phased development of new openings concurrent with adjacent lab operations is anticipated).

5. Make recommendations for follow-up geotechnical investigations after access to the mine has been restored, including tests to determine relevant rock properties and further geotechnical analyses to be the basis for detailed engineering design.

2.0 EXISTING GEOTECHNICAL DATA

Homestake rocks comprise a variety of metamorphic rock types subdivided into three distinct units: Poorman, Homestake, and Ellison formations, listed from oldest to youngest. The base of the Poorman Formation consists of metamorphosed tholeiitic basalt with possible back-arc basin affinities whereas the remaining Poorman lithologies are metasediments that include a complex succession of rock types (see Figure 2). The lowest known portion of the Poorman Formation as determined from diamond drilling and mapping is the Yates Unit. It largely comprises amphibolite. This unit is exposed at the surface in the Blacktail Gulch area north of Lead (see Figures 3 and 4) and continues down-plunge to the southeast through the core of the Lead Anticline.

The assessment of intact rock properties and rock mass properties that follows is based on very limited data at this time but it is deemed adequate to demonstrate the constructability of the underground laboratory rooms.

2.1 Intact Rock Properties

The only available rock property data is reported in publications by Pariseau et al.[10,11] and Tesarik et al[13].

Pariseau et al.[10] reported intact (laboratory) properties for the Homestake, Poorman and Ellison formations in their study of stope stability at the Homestake Mine. Tests were performed in selected orientations to investigate the anisotropy of the material. Reported results for the elastic properties and strength of the Poorman formation are presented in Table 1.

TABLE 1 – PROPERTIES OF POORMAN FORMATION

E_1(MPa)	E_2(MPa)	E_3(MPa)	ν_{12}	ν_{23}	ν_{31}	G_{12}(MPa)	G_{23}(MPa)	G_{31}(MPa)
32,267	22,753	27,303	0.20	0.17	0.15	11,445	10,480	12,755
σ_{c1}(MPa)	σ_{c2}(MPa)	σ_{c3}(MPa)	σ_{t1}(MPa)	σ_{t2}(MPa)	σ_{t3}(MPa)	-	-	-
69.0	94.0	84.6	5.7	20.6	13.2	-	-	-

2 and 3 directions are parallel to schistosity, 1 direction is perpendicular to schistosity

Although it does not seem intuitive that the modulus in the direction perpendicular to the foliation be higher than the moduli parallel to the foliation, the properties of the Poorman Formation showed only weak anisotropy and it is reasonable to conduct analyses assuming isotropic behaviour. Therefore, the intact elastic properties for the analysis of the excavations were selected as the average of the orthotropic properties:

E = 27,441 MPa, and $\nu = 0.17$. The isotropic shear modulus resulting from these values is given by $G = \frac{E}{2(1+\nu)} = \frac{27{,}441}{2(1+0.2)} = 11{,}727$ MPa, which is reasonably close to the average of the three shear moduli (11,560 MPa).

Tesarik et al.[13] reported modulus, uniaxial compressive strength and tensile strength estimates based on results from two unconfined compressive tests and five Brazilian tests performed on cores from a grab sample from the Yates formation. These values are reported as:

E = 100,000 MPa, σ_{ci} = 200 MPa, and σ_t = 13 MPa.

It is worth noting that the stress distributions around excavations calculated by three-dimensional elastic stress analyses are not dependent on the elastic modulus of the material, and only weakly dependent on Poisson's ratio for reasonable ranges for geological materials (0.15 to 0.35). For long prismatic excavations such as the drifts and the laboratory rooms, the stresses are independent of both modulus and Poisson's ratio. This is an important observation for reasons explained later in the discussion of the choice of the failure criterion.

2.2 In situ Stresses

Two sets of in situ stresses have been reported, one by Pariseau et al.[10], the other by Tesarik et al.[13]. Both sets are reported below and are fairly close to each other, however, the set reported by Tesarik et al. was selected for the analyses because it is based on measurements over a wider range of location depths. The set reported by Tesarik was based on a research study by Pariseau for the Bureau of Mines[11].

In situ stresses reported by Pariseau[10] et al. (6950L to 7100L):	***In situ stresses reported by Tesarick et al.[13] (3050L to 7400L):***
Metric:	
σ_V = 0.02828 z (m) MPa	σ_V = 0.02828 z (m) MPa
σ_{H1} = 14.33 + 0.01289 z (m) MPa	σ_{H1} = 14.33 + 0.01199 z (m) MPa
σ_{H1} = 0.834 + 0.01199 z (m) MPa	σ_{H1} = 0.834 + 0.01244 z (m) MPa
Imperial:	
σ_V = 1.25 z (ft) psi	σ_V = 1.25 z (ft) psi
σ_{H1} = 2078 + 0.57 z (ft) psi	σ_{H1} = 2078 + 0.53 z (ft) psi
σ_{H1} = 121 + 0.53 z (ft) psi	σ_{H1} = 121 + 0.55 z (ft) psi

Because both sets of in situ stresses report magnitudes only and no orientations (other than the vertical stress), numerical analyses will have to be run for more than one stress orientation.

2.3 Rock Mass Ratings and Choice of Failure Criterion

2.3.1 Tunnelling Quality Index, Q'

Tesarik et al.[13] reported the rock mass conditions at 3 sites in the Homestake Mine. Two of the sites reported are located in the Poorman and Homestake formations approximately at the 7400L. The third site is located at the 4850L and in the Yates unit. The following are the reported ratings for the evaluation of the Tunnelling Quality Index, Q':

Yates Unit	***Poorman Formation***
$RQD = 85$	$RQD = 75$
$J_n = 0.75$ (massive, no or few joints)	$J_n = 4$ (2 joint sets)
$J_r = 4$ (discontinuous joints)	$J_r = 1$ (smooth, planar)
$J_a = 0.75$ (tightly healed joints)	$J_a = 1$ (unaltered joint walls)

From the surface photographs (Figures 3 and 4), it appears that the Yates Unit exhibits at least 2 joint sets plus a random set. It is possible that these are not as evident at depth due to the reported tightly healed and discontinuous joints, however, we feel that a conservative position is warranted and the J_n rating should be revised to a value of 6. The ratings for the Poorman formation seem reasonable judging from the surface exposure (Figure 2).

When estimating values of Q' for determination of parameters for the purpose of numerical analyses, the ratings for water, J_w, and stress, SRF, should not be considered as the water and stress effects are addressed directly by the analyses. If these two ratings were not left out, there would be a double accounting of these factors. Therefore, the Q' index and the equivalent RMR are estimated to be (after correcting the J_n rating for the Yates Unit):

Yates Unit	***Poorman Formation***
$Q' = \frac{RQD}{J_n} \times \frac{J_r}{J_a} = \frac{85}{6} \times \frac{4}{.75} = 75.6$	$Q' = \frac{RQD}{J_n} \times \frac{J_r}{J_a} = \frac{75}{4} \times \frac{1}{1} = 18.8$
$RMR = 44 + 9 \times \ln Q' = 44 + 9 \times \ln 75.6 = 83$	$RMR = 44 + 9 \times \ln Q' = 44 + 9 \times \ln 18.8 = 70$

These values of RMR justify the choice of failure criterion presented in the next section and allow the estimation of the rock mass elastic moduli from the generally accepted relationships. Two relationships will be used in order get a reasonable level of confidence in the estimation of elastic modulus. One relationship is the latest proposed by Hoek and Diederichs[14] and is dependent on *RMR* (*RMR* = *GSI*) only, the other is dependent on both *RMR* and the intact (laboratory) elastic modulus and is based on the observation that the ratio of field modulus to intact modulus is equal to the square root of the ratio of field uniaxial compressive strength to intact strength, i.e.,

$$\frac{E_{rm}}{E_{lab}} = \sqrt{\frac{\sigma_{c\,rm}}{\sigma_{c\,lab}}}; \quad \frac{\sigma_{c\,rm}}{\sigma_{c\,lab}} = \sqrt{s}$$

$$\therefore$$

$$E_{rm} = E_{lab} \times s^{\frac{1}{4}}$$

Therefore:

Yates Unit

Hoek and Diederichs[14]:

$$E_{rm} = 100 \times \left(\frac{1 - D/2}{1 + e^{(75+25D-GSI)/11}} \right) = 67.4\ GPa$$

Calculation of parameter '*s*'[15]:

$$s = e^{\frac{RMR-100}{9-3D}} = e^{\frac{83-100}{9}} = 0.1512$$

Square root of field to intact strength ratio:

$$E_{rm} = E_{lab} \times s^{\frac{1}{4}} = 100 \times 0.1512^{\frac{1}{4}} = 62.4\ GPa$$

Poorman Formation

$$E_{rm} = 100 \times \left(\frac{1 - D/2}{1 + e^{(75+25D-GSI)/11}} \right) = 38.8\ GPa$$

$$s = e^{\frac{RMR-100}{9-3D}} = e^{\frac{70-100}{9}} = 0.0357$$

$$E_{rm} = E_{lab} \times s^{\frac{1}{4}} = 27.4 \times 0.0357^{\frac{1}{4}} = 11.9\ GPa$$

D = disturbance factor (assumed D = 0: undisturbed)[15]

While the estimates of modulus by the two methods agree reasonably well for the Yates Unit, it is obvious that the estimate based on "*RMR* only" overestimates the modulus of the Poorman formation (the estimate of the field modulus is higher than the laboratory value). This is typical for rocks with lower moduli because the contribution of the intact rock to the field modulus is no longer overshadowed by the joint fabric characteristics. For this reason, the approach of degrading the laboratory value to a field modulus is preferred.

2.3.2 Choice of Failure Criterion

Castro et al.[3,4,5,6] and Martin et al.[7,8] have conclusively demonstrated that, in low confinement zones (i.e., at and near the excavation boundaries), the (σ_1-σ_3) failure criterion, when applied to

the stress results from elastic analyses in moderately jointed (RMR values of ~70 or better), brittle rock masses at great depth or under high in-situ stresses, accurately estimates both the extent of the damaged zones (micro-cracking) and the extent of the plastic zones. Castro and McCreath[6] postulate that the movement of wedges and blocks along pre-existing, generally non-continuous discontinuities has only a minor effect on the initiation of fracturing or damage inside the rock mass, because the rock blocks do not initially have the kinematic freedom to allow translation or rotation. Therefore, the stress-induced damage process has to begin by fracturing through the blocks of intact rock inside the rock mass; for example, by breaking the rock bridges between the existing discontinuities (Castro[3]).

Fracturing begins by the nucleation and propagation of extension fractures within the intact rock. Extension fracturing (slabbing or spalling) is commonly observed to grow parallel to the excavation boundary. This means that the stress at which damage initiates in a moderately jointed rock mass is controlled by the behavioural characteristics of the intact rock, rather than by the behavioural characteristics of the discontinuities in the rock mass. Therefore, valid information can be extracted from laboratory tests on intact rock from which to assess the initiation of rock mass damage.

Potential DI (damage initiation) zones around deep excavations can be reliably predicted by performing elastic numerical analyses to identify regions where the deviatoric stress, $(\sigma_1 - \sigma_3)$, exceeds the damage initiation stress, σ_{DI}. This stress can be estimated by the threshold value at which stable crack growth commences for intact rock tested under uniaxial compression, σ_{sc} (Castro et al.[5]).

After damage to the intact rock has progressed sufficiently, macroscopic failure will eventually occur. However, the actual rock mass "peak" strength that is achieved, and the macroscopic modes of failure that are eventually displayed, are strongly influenced by the field loading system characteristics. Important system characteristics may include: confining stress, opening geometry (particularly radius of curvature of surfaces), loading system stiffness, loading rate, stress gradient, method of excavation, loading path, internal block geometry (i.e., presence of discontinuities), water and moisture conditions, scale effects, excavation methods, and the presence of rock support, amongst others (Castro et al.[4]).

Thus, as a working simplification, two threshold or trigger levels of stress (i.e., σ_{DI} and $(\sigma_c)_{sys}$) must be exceeded around an opening excavated in a moderately jointed brittle rock mass in order to first initiate damage within the intact material, and then to have the damage zones be exploited to failure.

Typical σ_{sc} values for hard rocks have been found in the range of 0.25 to 0.4 of the uniaxial compressive strength of the rock, σ_c. Therefore, extension fracturing is expected to occur between

0.3 to 0.4 of σ_c. The criterion for damage initiation through the intact rock material is then simply expressed as:

$$(\sigma_1 - \sigma_3) = 0.4\sigma_c$$

Application of this criterion has been shown to successfully predict the depth of the DI zones in the brittle, moderately jointed, norite rock mass surrounding the 2070 m deep Sudbury Neutrino Observatory (SNO) cavern in Sudbury (Castro et al.[5]).

Field observations of the actual lateral extent and depth of breakouts which have occurred around openings can be used to back-analyze the rock mass system strength, $(\sigma_c)_{sys}$, at the excavation surface, as proposed by Castro et al.[4]. This back-analysis approach consists of collecting observations of breakout dimensions and running an elastic back-analysis using the original tunnel (or drift) geometry at the location where the breakout was observed. The value of the mobilized peak system strength $(\sigma_c)_{sys}$ is then approximated by the value of the calculated tangential stress at the point where the final, stabilized breakout cuts the original excavation surface.

Application of this approach to the breakouts observed around different opening sizes excavated in the Lac-du-Bonnet granite at URL - AECL revealed that the rock mass system strength at the opening surface decreases for surfaces with increasing radius of curvature (Castro et al.[4]). For example, system strengths dropped from about 2 times σ_c for small radius (30 mm) to around 0.45 times σ_c for a 3.5 m diameter tunnel in a massive rock mass. Therefore for typical drift dimensions, $(\sigma_c)_{sys}$ should be about 0.5 to 0.6 of σ_c. The criterion for failure is then expressed as:

$$(\sigma_1 - \sigma_3) = 0.6\sigma_c$$

The advantage of this approach is that the only parameter required for the $(\sigma_1$-$\sigma_3)$ damage and failure criteria is the unconfined compressive strength of the intact rock, σ_c. In addition, because an elastic analysis is sufficient to establish micro-cracking initiation and plastic zones around excavations, the importance of the elastic parameters becomes of secondary importance.

3.0 NUMERICAL ANALYSES

Numerical analyses were conducted with Examine3D© (Rocscience, Inc.) for several stress orientations, mine locations (levels) and room layouts. Examine3D© is a boundary element code for the analysis of stress/displacements around excavations. The following variations of the stress, locations and layout options were considered in the analyses:

Room Layout:

Two room layouts were considered in the analyses. The first layout considered rooms laid out in a parallel pattern at 60 m centre to centre. The rooms are 20 m wide, resulting in a pillar of 40 m between rooms. The second layout comprised the same size rooms and spacing, but the rooms are laid out in an "en echelon" pattern (see Figure 1).

Location:

Three potential locations at the Homestake Mine have been considered:

1. 4850L (depth: 1480 m);
2. 7400L (depth: 2255 m); and
3. 8000L (depth: 2440 m)

The locations have a direct impact on the stress environment.

Stress Orientation:

The in situ stress measurements available in the literature for the Homestake Mine do not report orientations other than the vertical stress. Therefore, three orientations of the rooms with respect to the major horizontal stress were considered, namely:

1. the long axis of the rooms is aligned parallel to the major horizontal stress
2. the long axis of the rooms is aligned perpendicular to the major horizontal stress
3. the long axis of the rooms is aligned at 45° from the major horizontal stress

The combination of 2 layouts × 3 levels × 3 orientations results in 18 different analyses. In addition to these analyses, 2 extra analysis were run with tighter layouts. The parallel room layout at the 8000L with the rooms oriented perpendicular to the major horizontal stress was selected for the additional analyses. In the first analysis the distance between rooms was decreased by 25% (from 40 m to 30 m), and in the second analysis the distance between rooms

was decreased by 50% (from 40 m to 20 m) to determine at what spacing the rooms interfere with each other.

For each of the analysis mentioned above, three rooms were modelled in sequence. Each room was modelled in 4 stages (see Figure 5):

1. top heading (room size: 5 m wide × 5 m high at the centre)
2. slash sides leaving 2 m high side walls for access to roof by jumbo (room size: 16.87 m wide × 5 m high at the centre)
3. excavate middle bench – height to unsupported roof: 7 m (room size: 20 m wide × 10 m high at the centre)
4. excavate bottom bench (room size: 20 m wide × 15 m high at the centre)

The next two rooms were excavated in sequence, resulting in a total of 12 stages for each analysis. Figure 6 shows the second and third rooms in a parallel arrangement as well as the boundary element mesh for the final stage. Figure 7 shows the second and third rooms in an "en echelon" arrangement as well as the boundary element mesh for the final stage.

The sequence of excavation described above outlines one option to excavate the room, and does not necessarily mean that it is the only sequence or the optimum sequence. Optimization of the excavation sequence can be carried out once more details of the rock strength, fabric, and in situ stresses are obtained.

In addition, the analyses assume that in the chosen locations for the rooms, a single rock type is present and the rock mass is devoid of major faulting, shear zones and intrusions such as dykes. If any features of this nature are identified during the proposed geotechnical investigation, they should be addressed at the detailed design stage.

The adopted analyses naming convention is shown in Table 2.

TABLE 2 – ANALYSES NAMING CONVENTION

Layout	Level	Orientation	Filename	Stage - ××
Parallel	4850L	Parallel to $\sigma_{H\ maj}$	PAR-4850-LL-××.ex3	00 to 12
		Perpendicular to $\sigma_{H\ maj}$	PAR-4850-PP-××.ex3	00 to 12
		At 45° to $\sigma_{H\ maj}$	PAR-4850-45-××.ex3	00 to 12
	7400L	Parallel to $\sigma_{H\ maj}$	PAR-7400-LL-××.ex3	00 to 12
		Perpendicular to $\sigma_{H\ maj}$	PAR-7400-PP-××.ex3	00 to 12
		At 45° to $\sigma_{H\ maj}$	PAR-7400-45-××.ex3	00 to 12
	8000L	Parallel to $\sigma_{H\ maj}$	PAR-8000-LL-××.ex3	00 to 12
		Perpendicular to $\sigma_{H\ maj}$	PAR-8000-PP-××.ex3	00 to 12
		At 45° to $\sigma_{H\ maj}$	PAR-8000-45-××.ex3	00 to 12
En Echelon	4850L	Parallel to $\sigma_{H\ maj}$	ENE-4850-LL-××.ex3	00 to 12
		Perpendicular to $\sigma_{H\ maj}$	ENE-4850-PP-××.ex3	00 to 12
		At 45° to $\sigma_{H\ maj}$	ENE -4850-45-××.ex3	00 to 12
	7400L	Parallel to $\sigma_{H\ maj}$	ENE -7400-LL-××.ex3	00 to 12
		Perpendicular to $\sigma_{H\ maj}$	ENE -7400-PP-××.ex3	00 to 12
		At 45° to $\sigma_{H\ maj}$	ENE -7400-45-××.ex3	00 to 12
	8000L	Parallel to $\sigma_{H\ maj}$	ENE -8000-LL-××.ex3	00 to 12
		Perpendicular to $\sigma_{H\ maj}$	ENE -8000-PP-××.ex3	00 to 12
		At 45° to $\sigma_{H\ maj}$	ENE -8000-45-××.ex3	00 to 12
Parallel rooms 25% closer	8000L	Perpendicular to $\sigma_{H\ maj}$	PAR-8000-PP-12-25PCT.ex3	12
Parallel rooms 50% closer	8000L	Perpendicular to $\sigma_{H\ maj}$	PAR-8000-PP-12-50PCT.ex3	12

4.0 NUMERICAL ANALYSES RESULTS

Results for each numerical analysis were obtained at the excavation boundaries, at selected planes and in a voxel box around the first room for the evaluation of micro-cracking and plastic zones. The following selected planes were located as follows (see Figures 8 and 9):

1. 1 horizontal plane through mid-height of the rooms
2. 3 vertical planes, each along the long axis of each room
3. 1 vertical plane perpendicular to the axis of the rooms, at the beginning of the enlargement
4. 1 vertical plane perpendicular to the axis of the rooms, at the midpoint of the rooms
5. 1 vertical plane perpendicular to the axis of the rooms, at the blunt end of the rooms

The location and density of results in the voxel boxes is shown in Figure 10.

4.1 Spacing between Excavations

The elastic solution for a circular excavation in infinite medium suggests that the stress intensification due to the influence of the excavation, two diameters away from its edge, is down to within 4% of in situ stresses. Therefore, it is expected that for 20 m wide rooms and 40 m pillars between them, the influence of one excavation on the other will be negligible. This is confirmed by the numerical results for all layouts and stress orientations (see Figures 11 and 12). Figure 11 shows a comparison of σ_1 contours for the parallel room layout at the 8000L with spacings of 60 m (40 m pillar), 50 m (30 m pillar) and 40 m (20 m pillar). Figure 12 shows the profile of vertical stress along a line perpendicular to the long axes of the excavations at mid chamber and vertically located at the spring line.

Both the tangential stress (σ_1) contours and the profile of vertical stress show that a spacing of 60 m c/c between the excavations results in negligible interference between the rooms (~ 2% change in tangential stress at the springline). Decreasing the spacing between the rooms by 25% results in a 4% increase in tangential stress at the springline of the rooms, and further decreasing the spacing between the rooms by 50% results in a 9% increase in tangential stress at the springline of the rooms.

The implications of these stress magnifications for the closer spacing of the rooms are more significant in the Poorman formation than in the Yates unit. This is because the strength of the Yates formation is such that the depth of the plastic zone is very small and does not compromise the pillars between the rooms. However, in the Poorman formation the extent of the plastic zone is more substantial at the 7400L and the 8000L and the vertical overstress around the rooms will transfer into the core of the pillar potentially extending the failed zone to a significant portion of

the pillar. Therefore, it is recommended that the proposed spacing of 60 m c/c between rooms be adopted.

4.2 Orientation of Excavations

The main driving stresses in failure of underground openings are tensile stresses and shear or deviatoric stresses. Crushing under uniform (spherical) stress is rarely seen except for very high stress environments in very weak porous material, where the rock structure may collapse. In the case of the excavations for the laboratory rooms, due to the proposed depths and shape of the openings, the stress environment is mostly compressive. Therefore, the driver for failure is the deviatoric stress. In situ stresses become magnified around excavations due to concentration of stresses as they flow around them. The stress magnification factors are a function of the shape of the openings, and in the case of the proposed excavations (10 m high side walls and 20 m wide room), the tangential stresses (σ_θ) in the side walls are expected to be of the order of:

$$\sigma_\theta = 2.5\sigma_V - 0.9\sigma_H$$

where, σ_V is the in situ vertical stress and σ_H is the in situ horizontal stress perpendicular to the excavation long axis. This means that the preferred orientation of the laboratory rooms is the one with the long axis perpendicular to the major horizontal in situ stress in order to minimize the stress concentration in the walls. The roof and floor of the rooms do not pose concerns as the in situ stresses and the shape of the openings are in favourable orientations.

These observations are confirmed by the results of the numerical analyses. Figure 13 shows the tangential stresses at the excavation boundaries for rooms with the long axis oriented parallel, perpendicular and at 45° to the major horizontal stress. Although the stress differences between the three orientations are small (~12 MPa), it is clear that the most favourable orientation, from a stress minimization viewpoint, is that with the long axis of the excavations perpendicular to the major horizontal stress.

In the case of the Poorman formation, this result has to be taken with caution because the rock exhibits a moderate strength anisotropy and the best orientation for the excavations is perpendicular to the schistosity. The best case scenario for the Poorman formation would be one where the major horizontal stress is parallel to the schistosity, and the rooms driven perpendicular to both, thus taking advantage of the stronger orientation of the rock and the smallest stress intensification. The effect of orientation on the plastic zones and the damage initiation zones (micro-cracking) for the Poorman formation and the Yates unit at different depth is shown in Figures 14 through 19.

4.3 Depth of Excavations

The choice of the location for the neutrino laboratory rooms is driven by scientific needs considerations. The current proposed locations result in levels of vertical stress that vary between approximately 42 MPa and 69 MPa with a corresponding range of major horizontal stress between 32 MPa and 44 MPa. The implication of these stress level ranges is that the in situ deviatoric stress (driving force behind failure) increases from approximately 10 MPa at the 4850L to 25 MPa at the 8000L. This means that the Poorman formation cannot sustain the stresses at the 7400L and 8000L without the development of large zones of failed ground and the need for major support. The Yates formation will experience only modest zones of plasticity on the side walls at the 7400L and 8000L after excavation of the lower bench and will remain within its elastic range at the 4850L.

Figures 20 and 21 show the extent of the micro-cracked zones and the failed zones, respectively, in the Yates unit. These figures show that the Yates unit will present no problem at the 4850L (no plasticity or micro-cracking) and limited zones of plasticity at the 7400L and 8000L on the side walls (2.5 m or less). Damage (micro-cracking) is also limited to the side walls and the end wall of the excavation.

Figure 22 shows that the extent of the plastic zone in the Poorman formation at the 4850L is also limited to the sidewalls, but is considerably larger at the 7400L and 8000L reaching deep into the rock (6 or 7 m).

4.4 Rockburst Potential

Of the two proposed rock types for the location of the laboratory rooms, the Yates unit will pose the most difficulty with rock bursting. The conditions for rock bursting are the combination of high stress, strong rock and brittle behaviour. All of these conditions are met at the 7400L and the 8000L in the Yates unit. The intact modulus of the Yates unit has been reported as 100 GPa, and even when down-graded to field conditions it is still of the order of 65 GPa. The laboratory uniaxial tests in the two samples of the Yates unit were reported to show elastic-brittle behaviour, which means that all the strain energy stored in the rock is released suddenly, without a phase of slow energy dissipation associated with a damage process.

The Poorman formation has lower strength than the Yates unit but it is more deformable, thus storing more strain energy. However, this strain energy is expended in the process of failing and damaging the rock. In addition, the rock in the Poorman formation has not been described as a brittle rock. Laboratory testing in the geotechnical investigation phase of the project should characterize the bursting propensity of the Poorman formation.

The strain energy density stored in the rock can be represented by the stress state and the elastic properties of the rock:

$$w = \frac{\sigma_1^2 + \sigma_2^2 + \sigma_3^2 - 2\nu(\sigma_1\sigma_2 + \sigma_2\sigma_3 + \sigma_3\sigma_1)}{2E}$$

where w is the strain energy density (e.g., J/m^3), σ_i (e.g., MPa) are the principal stresses and E (e.g., MPa) is the elastic modulus. Plots of the strain energy density stored around the excavation in the Yates unit compared to the extent of the plastic and micro-crackedd zones is shown in Figures 23 and 24.

The figures show that the side walls of the excavations have a considerable amount of strain energy stored in them and although a portion of that energy will be spent in the process of damaging the rock before failure, the likelihood of strain bursts is high. While strain bursting does not compromise stability, it crates a risky environment during development.

When designing support for the walls, consideration should be taken to implement a support system which can absorb sudden releases of energy without failing (e.g. cables with partially de-bonded sections, or large deformation cone bolts). At the development stage of excavation, a de-stress blasting program may have to be implemented to relieve the zones of potential high energy. De-stress blasting involves drilling boreholes into zones of anticipated high stress conditions prior to excavation and blasting using a powder factor that will not cause excessive damage to the subsequent excavation. The blasting "pre-conditions" the ground by creating fractures within the rock mass and "softens' the ground by transferring it from the elastic-brittle failure behaviour to a plastic form of deformation. De-stress blasting is as much of an art as a science, and a unique de-stress drilling and blasting pattern may have to be derived for each excavation shape, rock type and anticipated stress condition. A reference paper on a state-of-the-art review of de-stess blasting practice in hard rock mines by Mitri and Saharan[17] has been included as Appendix C.

4.5 Ground Support

The Q' values reported in Section 2.2.1 must be now adjusted for the water and stress conditions for use in support charts (Figures 31 through 34). Dry conditions or minor inflows are reported in the available literature and as such, J_w is set to 1 for all locations. Q values for the Poorman formation and the Yates unit for the 4850L and 7400L/8000L are shown below:

SIDE WALLS

Yates Unit – 4850L

$$\frac{\sigma_c}{\sigma_1} = \frac{200}{42} = 4.8 \quad \rightarrow \quad SRF = 5$$

$$Q = \frac{RQD}{J_n} \times \frac{J_r}{J_a} \times \frac{J_w}{SRF} = \frac{85}{6} \times \frac{4}{.75} \times \frac{1}{5} = 15.1$$

Poorman Formation – 4850L

$$\frac{\sigma_c}{\sigma_1} = \frac{90}{42} = 2.1 \quad \rightarrow \quad SRF = 12$$

$$Q = \frac{RQD}{J_n} \times \frac{J_r}{J_a} \times \frac{J_w}{SRF} = \frac{75}{4} \times \frac{1}{1} \times \frac{1}{12} = 1.6$$

Yates Unit – 7400L and 8000L

$$\frac{\sigma_c}{\sigma_1} = \frac{200}{64-69} = 2.9-3.1 \quad \rightarrow \quad SRF = 6$$

$$Q = \frac{RQD}{J_n} \times \frac{J_r}{J_a} \times \frac{J_w}{SRF} = \frac{85}{6} \times \frac{4}{.75} \times \frac{1}{9} = 8.4$$

Poorman Formation – 7400L and 8000L

$$\frac{\sigma_c}{\sigma_1} = \frac{90}{64-69} = 1.3-1.4 \quad \rightarrow \quad SRF = 20$$

$$Q = \frac{RQD}{J_n} \times \frac{J_r}{J_a} \times \frac{J_w}{SRF} = \frac{75}{4} \times \frac{1}{1} \times \frac{1}{20} = 0.9$$

ROOF – Long Axis of Excavation Perpendicular to Major In Situ Horizontal Stress

Yates Unit – 4850L

$$\frac{\sigma_c}{\sigma_1} = \frac{200}{32} = 6.3 \quad \rightarrow \quad SRF = 1.5$$

$$Q = \frac{RQD}{J_n} \times \frac{J_r}{J_a} \times \frac{J_w}{SRF} = \frac{85}{6} \times \frac{4}{.75} \times \frac{1}{1.5} = 50.4$$

Poorman Formation – 4850L

$$\frac{\sigma_c}{\sigma_1} = \frac{90}{32} = 2.8 \quad \rightarrow \quad SRF = 9$$

$$Q = \frac{RQD}{J_n} \times \frac{J_r}{J_a} \times \frac{J_w}{SRF} = \frac{75}{4} \times \frac{1}{1} \times \frac{1}{9} = 2.1$$

Yates Unit – 7400L and 8000L

$$\frac{\sigma_c}{\sigma_1} = \frac{200}{41-44} = 4.5-4.9 \quad \rightarrow \quad SRF = 2$$

$$Q = \frac{RQD}{J_n} \times \frac{J_r}{J_a} \times \frac{J_w}{SRF} = \frac{85}{6} \times \frac{4}{.75} \times \frac{1}{2} = 37.8$$

Poorman Formation – 7400L and 8000L

$$\frac{\sigma_c}{\sigma_1} = \frac{90}{41-42} = 2.1-2.2 \quad \rightarrow \quad SRF = 12$$

$$Q = \frac{RQD}{J_n} \times \frac{J_r}{J_a} \times \frac{J_w}{SRF} = \frac{75}{4} \times \frac{1}{1} \times \frac{1}{12} = 1.6$$

The actual roof span and the side wall heights have to be adjusted to equivalent spans depending on the use of the rooms (excavation category). This is accomplished by multiplying the actual span by the excavation support ratio (ESR). The ESR for large civil caverns is unity (1) and as such, the excavation dimensions remain unchanged, i.e., the roof span is 20 m and the side walls height is 10 m.

In addition to these empirical estimates for support, the extent of the micro-cracked and plastic zones from the numerical analyses will be used to corroborate the empirical estimates and to determine support length. Figures 25 through 27 show the depth of the micro-cracked and plastic zones at the 4850L and the depth of the plastic zones at the 7400L in the Poorman formation. Figures 28 through 30 show the depth of the plastic zones at the 4850L and the depth of the micro-cracked and plastic zones at the 8000L in the Yates unit.

Table 3 shows the preliminary support recommendations for the excavations at the Homestake mine.

TABLE 3 – PRELIMINARY SUPPORT RECOMMENDATIONS

FORMATION	LEVEL	LOCATION	BOLTING	SHOTCRETE
Poorman Formation (see Figures 31 and 32)	4850L	Roof	5 m long bolts @ 2 m c/c	90 mm fibre reinforced shotcrete
		Side Walls	8 m long bolts @ 1.75 m c/c	100 mm unreinforced shotcrete
	7400L/8000L	Roof	5 m long bolts @ 1.75 m c/c	100 mm fibre reinforced shotcrete
		Side Walls	8 m long bolts @ 1.5 m c/c	90 mm fibre reinforced shotcrete
Yates Unit (see Figures 331 and 34)	4850L	Roof	5 m long spot bolts	none
		Side Walls	4 m long bolts @ 2.5 m c/c	none*
	7400L/8000L	Roof	5 m long bolts @ 2.5 m c/c	none
		Side Walls	4 m long bolts @ 2.25 m c/c	50 mm* unreinforced shotcrete

* - The excavation walls should be protected from long term deterioration by at least a layer of 50 mm of fibre reinforced shotcrete

5.0 RECOMMENDATIONS

5.1 Excavations

These recommendations are the result of the interpretation of the numerical analyses and the current understanding of the rock mass characteristics and in situ state of stress:

1. The proposed spacing between the laboratory rooms is verified as appropriate and it should not be reduced, especially at the deeper locations.

2. Both the parallel and the 'en echelon' room layouts are viable as long as the recommended spacing between the rooms is respected.

3. Rooms in the Yates unit should be oriented with their long axis oriented perpendicular to the major horizontal in situ stress. Rooms in the Poorman formation should be oriented with their long axis oriented perpendicular to the foliation to take advantage of the stronger orientation of the rock.

4. If possible, rooms developed at the deeper levels should be located in the Yates unit.

5. Rooms should be excavated in three (3) benches with the top bench being excavated in two steps, a centre heading and side slashes leaving 2 m high side walls for access to roof by jumbo (room size: 16.87 m wide × 5 m high at the centre).

6. Design of the support for the side walls should take into consideration the potential for the development of strain bursts. This means that the support should have the capacity to absorb sudden energy released by the failure of the rock. The excavation walls should be protected from long term deterioration by at least a layer of 50 mm of fibre reinforced shotcrete.

7. It can be expected that variability of the rock mass strength will impact local design and support requirements.

It should be noted that the analysis carried out and support recommendations are based on the assumption that all excavation is being carried out in fresh rock, once the mine has been de-watered to the selected laboratory level. Following de-watering of the mine, it is probable that an extensive rehabilitation and re-supporting of the existing mine workings and mine access-ways will be required to replace and update potentially aged and corroded support. During the process of dewatering there is the possibility of destabilization of areas within the once flooded workings as a result of excess pore water pressure within the rock mass surrounding the openings. This

will depend on how quickly the water pressure can dissipate as the workings are de-watered. One important consideration during mine de-watering will be to identify, characterize and monitor any mining zones that have been backfilled or bulkheaded, subsequently flooded, and then de-watered. Excess water pressure within the backfill or behind bulkheads can potentially lead to failure with subsequent backfill or water mobilization.

5.2 Follow-up Geotechnical Investigations

After access to the mine has been restored, and in light of the findings from the numerical analyses of the excavations for the laboratory rooms, the recommendations for a follow-up geotechnical investigation program are:

1. Conduct an underground face/drift mapping program at the proposed potential locations for the Neutrino laboratory rooms, namely, at 4850L, 7400L and 8000L levels. Mapping should include measurement of all parameters required for Bieniawski's Rock Mass Rating as well as NGI – Tunnelling Quality Index, Q. In addition, definition of joint fabric, including measurements of joint orientations will be required for use in stereographic projection analyses. Mapping and joint fabric definition should be conducted at selected locations for each rock type. Particular attention should be paid to the rock mass quality near the contact between different rock types as often these contacts exhibit poorer conditions.

2. Establish a drilling program to obtain core for the purpose of rock mass characterization, hydrogeological characterization, selection of samples for a laboratory testing program, and for an in-situ stress measurement program:

    a. Rock Mass Characterization – measurement of RQD values, estimation of UCS values and further characterization of joint conditions (in addition to the face/drift mapping program).

    b. Hydrogeological Characterization – a program of packer tests for the estimation of rock mass permeability should be established for each rock type and at the three proposed horizons. The de-watering programs that will be necessary to establish access to the deeper levels should also contribute to the understanding of the hydrogeology of the mine.

    c. Laboratory Testing Program – A laboratory testing program consisting of uniaxial compression tests, Brazilian tests, and triaxial tests at prescribed confinements for each rock type for the estimation of elastic properties and strength parameters. It is important that the post-peak behaviour of the rocks be characterized in order to

establish the potential for rock bursting. In addition, sets of direct shear tests at 3 or 4 prescribed confinements on joints of each identified set, for each rock type should be carried out for definition of joint peak and residual strengths.

d. In Situ Stress Testing Program – Stress testing to obtain the three-dimensional stress field, including orientations, is important for proper orientation of the laboratory rooms. This requires a minimum of 3 borehole orientations when using USBM stress cells, and 3 to 5 measurements per hole to ensure success. If CSIRO stress cells are used, the three-dimensional stress field can be obtained from a single hole, however, the success of the tests can only be verified after the cells are over-cored and the epoxy inspected for good connectivity of the cell to the rock. Because the CSIRO cells are not re-usable, it would be required that enough cells are ordered assuming a success rate for the tests. The rock at the proposed locations of the Homestake mine is of reasonably good quality and is not expected to be problematic for the performance of stress testing. Stress tests should be carried out at the different rock types as it is plausible that they may have different stress regimes.

GOLDER ASSOCIATES LTD.

Original signed by:

C. M. Steed, P. Eng.
Principal

Original signed by:

J. L. Carvalho, Ph. D., P. Eng.
Associate

JLC/CMS/ms

n:\active\2006\1117\06-1117-014 - lbn laboratory - neutrino - south dakota\final report\06-1117-014 06may30 finalreport.doc

REFERENCES

[1] T. J. Campbell, Synopsis of the Homestake Mine Geology, November, 2005, http://homestake.sdsmt.edu/Geology/geology.htm

[2] T. J. Campbell, Characteristics of the Yates Unit Amphibolite, November, 2005, http://homestake.sdsmt.edu/Geology/geology.htm

[3] Castro, L.A.M. (1996). Analysis of Damage Initiation around Deep Openings Excavated in a Moderately Jointed Rock Mass. Ph. D. thesis, Department of Civil and Rock Mechanics Eng., U. of Toronto, Ontario, Canada.

[4] Castro, L.A.M.; McCreath, D. and Kaiser, P.K. (1995). Rock Mass Strength Determination from Breakouts in Tunnels and Boreholes. 8th ISRM Congress, Tokyo: 531-536.

[5] Castro, L.A.M.; McCreath, D.R. and Oliver, P. (1996). Rock Mass Damage Initiation Around the Sudbury Neutrino Observatory Cavern. 2nd North American Rock Mechanics Symposium, Aubertin, Hassani & Mitri (eds), Balkema, Montreal, 2: 1589-1595.

[6] Castro, L.A.M. & McCreath, D.R. (1997). How to Enhance the Geomechanical Design of Deep Openings? 99th CIM Annual Meeting, CIM'97, Vancouver, Canada.

[7] Martin, C.D. & Chandler, N.A. (1994). The progressive fracture of Lac-du-Bonnet granite. Int. J. Rock Mech. Min. Sci. & Geomech. Abst., 31(6): 643-659.

[8] Martin, C.D. and Read, R.S. (1996). AECL's Mine-by Experiment: A test tunnel in brittle rock. 2nd North American Rock Mechanics Symposium, Montreal. Balkema, 1: 13-24.

[9] Pariseau, W.G., Duan, F., and Schmuck, C.H., 1984, Numerical Assessment of the Influence of Anisotropy on Steeply Dipping VCR Stopes, in Pariseau, W.G., ed., Geomechanics Applications in Underground Hardrock Mining, American Institute of Mining, Metallurgical, and Petroleum Engineers, p. 39-63.

[10] Pariseau, W. and Duan, F., Stope Stability as a Function of Depth at the Homestake Mine. Undated.

[11] Pariseau, W., 1985. Research Study on Pillar Design for Vertical Crater Retreat (VCR) Mining. Bureau of Mines Contract Report J0215043, Oct.

[12] Pariseau, W. and Duan, F., and Schmuck, C.S., 1987. Stability Analysis of the VCR Stope at the Homestake Mine. Gold Mining 87, pp. 199-213.

[13] Tesarick, D., Johnson, J., Zipf, Jr., K, and Lande., K., 2002. Initial Stability Study of Large Openings for the National Underground Science Laboratory at the Homestake Mine, Lead, SD. Proceedings of the 5th North American Rock Mechanics Symposium and the 17th Tunnelling Association of Canada Conference: NARMS-TAC 2002, Hammah et al. (eds) Toronto, Ontario, Canada, 7-10 July 2002, pp.157-163.

[14] Hoek, E. and Diederichs, M.S., 2005, Estimation of Rock Mass Modulus, submitted for publication in the International Journal of Rock Mechanics and Mining Sciences, 14 p.

[15] Hoek E, Carranza-Torres CT, Corkum B. Hoek-Brown failure criterion – 2002 edition. Proceedings of the 5th North American Rock Mechanics Symposium and the 17th Tunnelling Association of Canada Conference: NARMS-TAC 2002, Hammah et al. (eds) Toronto, Ontario, Canada, 7-10 July 2002, pp.267-273.

[16] Grimstad, E. and Barton, N., 1993, Updating the Q system for NMT. Proceedings of the International Symposium on Sprayed Concrete: Modern Use of Wet Mix Sprayed Concrete for Underground Support, Oslo: Norwegian Concrete Association.

[16] Mitri, H.S. and Saharan, M.R., 2006, Destress Blasting in Hard Rock Mines – A State of the Art Review, CIM Bulletin, December 2005/January 2006.

JLC/CMS/ms

n:\active\2006\1117\06-1117-014 - lbn laboratory - neutrino - south dakota\final report\06-1117-014 06may30 finalreport.doc

FIGURES

APPENDIX A

INITIAL STABILITY STUDY OF LARGE OPENINGS FOR THE NATIONAL UNDERGROUND SCIENCE LABORATORY AT THE HOMESTAKE MINE, LEAD – TESARICK, D., JOHNSON, J., ZIPF, JR., K, AND LANDE., K., 2002

NARMS-TAC 2002, Hammah et al. (eds) © 2002 University of Toronto, ISBN 0 7727 6708 4

Initial stability study of large openings for the national underground science laboratory at the Homestake mine, Lead, SD

Doug Tesarik, Jeff Johnson, and Karl Zipf, Jr.
Spokane Research Laboratory, National Institute for Occupational Safety and Health, Spokane, WA USA
Kenneth Lande
University of Pennsylvania, Philadelphia, PA USA

ABSTRACT: The study of neutrinos—particles infinitesimally smaller than atoms—would be significantly advanced if a deep underground facility were available that would filter out unwanted cosmic radiation. Encouraging progress has been made in satisfying the criteria for such a facility with the selection of the Homestake Mine in Lead, SD, by the National Underground Laboratory Committee as the recommended site for a National Underground Science Laboratory (NUSL). The Homestake Mine is America's oldest and deepest underground mine, and its well-maintained infrastructure to depths of 2438 m below the surface makes the mine an excellent site for such a laboratory. The investigation reported here is an initial study of the stability of the first of the proposed chambers. A cylindrical room with a dome-shaped roof and floor was analyzed in three dimensions using the finite-difference program FLAC3D. The results were compared to recommended support requirements based on Barton's Tunneling Quality Index, Q. Based on model results and observations from previous mining studies, large rooms with 50-m roof spans can be constructed and will remain stable at 2141 m below the surface in the Poorman Formation when the rock is reinforced with cable bolts. Construction may be possible at lower levels in the Yates Formation if more extensive laboratory strength tests confirm initial results.

1. INTRODUCTION

Observation of solar neutrinos began in 1965, when Raymond Davis installed a 600-ton detector at the 4850 level of the Homestake Mine in Lead, SD [1]. From that beginning, neutrino astrophysics has grown into a worldwide research effort. There are large underground laboratories at Gran Sasso in Italy, Baksan in Russia, Kamioka in Japan, and Sudbury in Canada. Although there are U.S. participants in these experiments, until now, U.S. scientists have not been able to follow up on the original work by Davis at a U.S.-based facility. The end of gold mining at the Homestake Mine in December 2001 has provided a unique opportunity for the creation of what would be the deepest and largest underground laboratory in the world. The great thickness of overburden would filter unwanted cosmic radiation, allowing neutrinos to to be "captured" for study.

The primary reason for this growing interest in neutrinos is that understanding their properties is important to answering many cosmological and astrological problems, such as why the neutrino flux emitted by the Sun as a result of nuclear fusion is less than expected, the processes involved during the collapse of a massive star into a neutron star and associated supernova emissions, proton decay, and dark matter.

Among the proposals for a National Underground Science Laboratory (NUSL) is one for a one-million-ton water Cerenkov detector that would be about 20 times the size of the largest present detector, SuperKamiokande in Japan. The proposed Cerenkov detector would consist of 10 cylindrical modules each 50 m in diameter and 50 m high located between the 6950 and 7100 levels of the Homestake Mine in the Yates Formation. (Most mining has been in the Poorman and Homestake formations.) The investigation reported here is an initial study of the stability of the first of 10 proposed chambers and the first step in ensuring the safety of miners during excavation. A cylindrical room with a dome-shaped roof and floor was analyzed in three dimensions using the finite-difference program FLAC3D [2]. The results were compared to recommended support requirements based on Barton's Tunneling Quality Index, Q [3, 4].

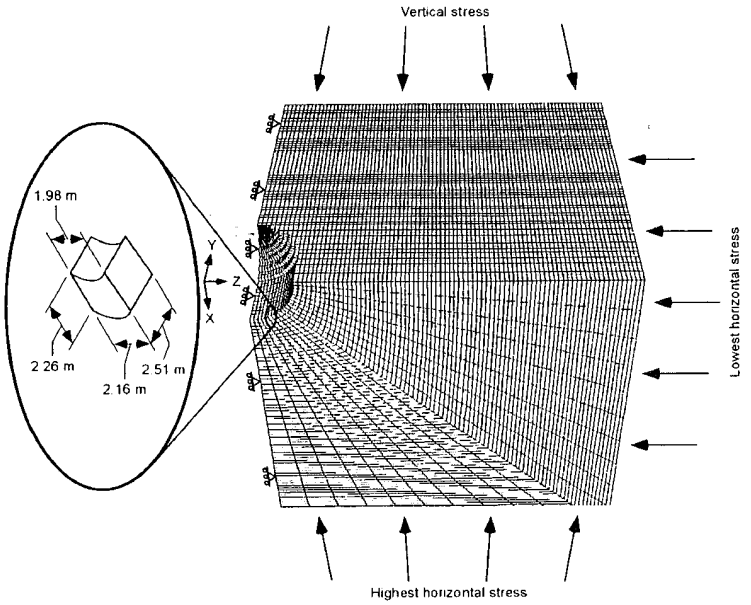

Figure 1.—Finite-difference mesh with excavation in one-eighth symmetry.

2. COMPUTER MODEL AND PREDICTED RESPONSE

The modeled room was a 50-m-high cylinder with 50-m-diameter hemispheres representing the mine roof and floor and a volume of 163,624 m^3. One-eighth symmetry was used to reduce the size of the finite-difference mesh, which consisted of 140,800 zones shaped like extruded annulus sectors having a 2.3-m radial thickness and an extruded length of 2.5 m (fig. 1). Sector dimensions were reduced to approximately 1.5 m for one computer run to confirm that the mesh size was small enough to estimate the depth of failure into the rock mass. The initial in situ state of stress used in these analyses was based on stress measurements made in the 1970's through 1980's at the Homestake Mine. Measurements between 930 and 2256 m in the mine resulted in a linear stress formula (Eq. 1) dependent on depth below the mine surface [5]. The initial stress state in the model was achieved by applying the three orthogonal stresses at the finite-difference mesh boundary seven radii from the rib of the cylindrical room and iterating to equilibrium.

$$\sigma_v = 28.28\ h,$$
$$\sigma_{h1} = 14{,}327.8 + 11.99\ h,$$
and $$\sigma_{h2} = 834.3 + 12.44\ h, \qquad \text{(Eq. 1)}$$

where h = depth in meters,
σ_v = vertical stress in kilopascals (kPa),
and σ_{h1} and σ_{h2} = horizontal stresses in kPa.

The room was assumed to be excavated in a homogenous, isotropic rock mass constructed between existing levels below 2118 m. The average depth between levels was used for parameter h (Eq. 1) to calculate initial stresses. A Mohr-Coulomb failure criterion defined by cohesion and angle of internal friction was used to limit the elastic behavior of the material or the strength of the rock mass. Because there was a limited amount of material property information on the Yates Formation, three values for cohesion were used—12.2, 18.3, and 24.4 MPa. These values represent 50%, 75%, and 100% of average strengths calculated from unconfined compressive strength test results conducted on specimens from the Poorman Formation and a value of 30° for the angle of internal friction. The field-scale unconfined compressive and tensile strengths in the Poorman Formation (42.3 and 6.58 MPa, respectively) were 50% of the average laboratory values. They were obtained by monitoring the loss of borehole extensometer anchors during mining of large vertical crater retreat stopes between 2118 and 2164 m at the Homestake Mine [6]. These extensometers were also used to calibrate a three-dimensional, finite-element program, resulting in a field-scale modulus of deformation equal to

23,615 MPa, or 25% of average laboratory values. This value was used in the finite-difference analyses.

Two specimens were prepared for unconfined compression tests and five specimens were prepared for Brazilian tensile tests from a grab sample of rock from the Yates Formation measuring approximately 1 by 0.5 m. The average tensile strength of these specimens was about the same as the average tensile strength of rock from the Poorman Formation, but the unconfined compressive strength was more than two times the values for the Poorman Formation. This implies that 24.4 MPa is about half the cohesion value for the Yates Formation and, based on these tests, is a reasonable estimate of the field, or rock mass, value of cohesion. It is important to emphasize that these specimens may not represent the entire Yates Formation. A thorough site investigation is essential to characterizing the rock more accurately. The high strength of the laboratory specimens combined with their elastic-brittle behavior when loaded to failure indicate that Yates rock may be prone to bursting.

Results from the finite-difference model indicate that the maximum depth of failure into the rock around the cavity is 10 m and occurs in the lower roof (fig. 2*S*). The maximum yield width in the room's rib is 6.8 m. Yield zones in the y-z plane through the origin are similar in shape, but not as extensive as yield zones in the x-y plane. If the centroid of the chamber is located 2141 m below the surface in rock equal in strength to that of the Poorman Formation, the model calculates yield zones in both the lower roof and ribs (fig. 2*A*). Previous mining experience confirms that a stope 24 m wide, 30 m long, and 46 m high excavated with the vertical crater retreat method at 2141 m suffered some caving, but remained open when the roof was supported with cable bolts [6]. Conversations with mine personnel indicated that large structures (45.7 m high, wide, and long) have been excavated, but are unstable at depths of 2416 m. These observations, combined with the finite-difference results, imply that 2141 m may be the deepest opening that can exist in the Poorman or Homestake formations without encountering stability problems (figs. 2*A*, *S*). However, if the rock strength of the Yates Formation is approximately twice that of the Poorman Formation, as initial laboratory tests indicate, then failure will be limited around the room constructed in Yates rock even at 2416 m underground (fig. 2*U*). Results could differ if the Yates rock has anisotropic material properties.

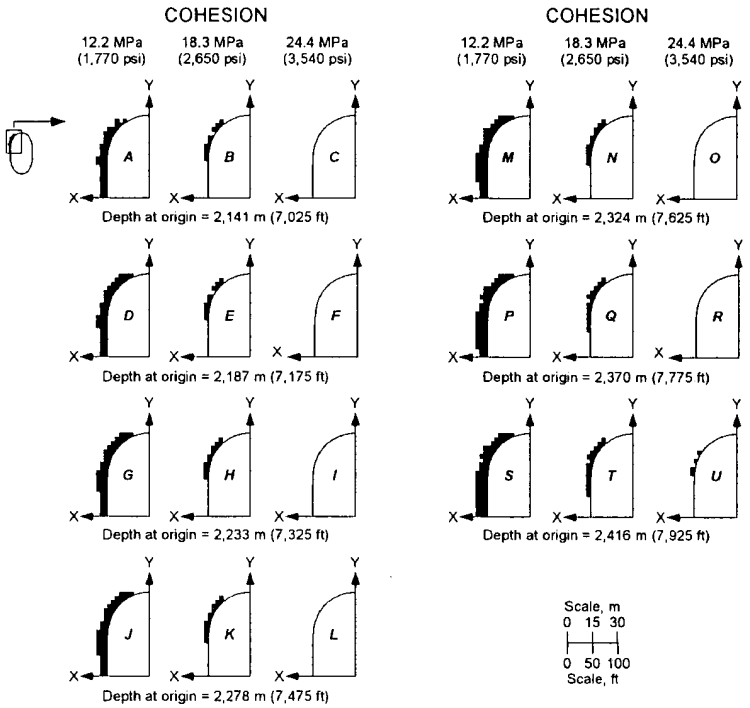

Figure 2.—Failure zones in x-y plane through the origin.

Failure zones were initiated where redistributed stresses became concentrated near the lower roof of the chamber and propagated into the ribs as mining depth increased. The thickness of the failure zone diminished to zero near the apex of the hemispherical roof because the arched opening eliminated a wedge of material of a type that often fails and requires support.

3. ROCK MASS CLASSIFICATION

A comparative rock mass characterization using Q (Eq. 2) was performed with data obtained from three locations at the Homestake Mine to determine if the support recommendations from this system could be reasonably applied to the large chamber proposed in the Yates Formation. Geomechanics data were collected at three different sites.

$$Q = RQD/J_n \times J_r/J_a \times J_w/SRF \qquad \text{(Eq. 2)}$$

where Q = tunneling quality index,
RQD = rock quality designation,
J_n = joint set number,
J_r = joint roughness number,
J_a = joint alteration number,
J_w = joint water reduction factor,
and SRF = stress reduction factor.

Site 1 is located 2118 m underground in rock primarily of the Homestake Formation, although a small amount of Poorman rock is present. Some areas are fractured, presumably from high stress caused by nearby stoping. Steeply dipping bedding planes are the major discontinuity at this site. The bedding planes are tightly healed; however, in highly stressed areas, the spacings between open bedding planes is 5 to 10 cm. These bedding planes are discontinuous, and most of them can not be traced more than 1 m. Occasionally, joints with random orientations were observed. These joints are tight and smooth, contain no filling material, and can be traced for 3 to 6 m. The estimated number of bedding planes, joints, and fractures per cubic meter was 16.

Site 2 is located 2141 m below the surface in the Homestake and Poorman formations. The area is heavily jointed. Steeply dipping bedding planes are spaced 15 to 30 cm apart and, similar to rock at site 1, stress redistributed from nearby stopes has opened up discontinuities that were otherwise tightly healed. One poorly developed joint set was observed that had a spacing of about 30 cm and a continuity of 3 to 6 m. These fractures are tight and rough, and contain a hard filling. The estimated number of bedding planes, joints, and fractures per cubic meter was 12.

Site 3 is 1508 m deep in the Yates Formation, the proposed host rock for the NUSL. Site 3 rock is massive with no or few joints. The estimated number of bedding planes, joints, and fractures per cubic meter was less than 4.

The RQD of the rock at these sites was estimated from the number of joints per cubic meter. All sites were dry. Laboratory unconfined compressive strengths of the intact rock used to calculate the stress reduction factor were 84.6 MPa for sites 1 and 2, and 186 MPa for site 3. Vertical stress (Eq. 1) was used as the major principal stress because three out of four in situ stress measurements at the mine indicated that the major principal stress direction aligned with the vertical [5].

On the basis of empirical charts developed by Barton et al. [3] (fig. 3) and Grimstad and Barton [4] (fig.4), the recommended support for all three sites agreed well with the support used at these sites (table 1), indicating that it is reasonable to apply these charts to the large chamber proposed at the Homestake Mine (table 2).

The Grimstad and Barton chart recommends systematic bolting with 40 to 50 mm of unreinforced shotcrete for 25- and 50-m spans. The Barton chart recommends tensioned bolts with 2- to 3-m spacings for these spans. There are no support recommendations for spans exceeding 70 m because the plotted data exceed the range of the charts.

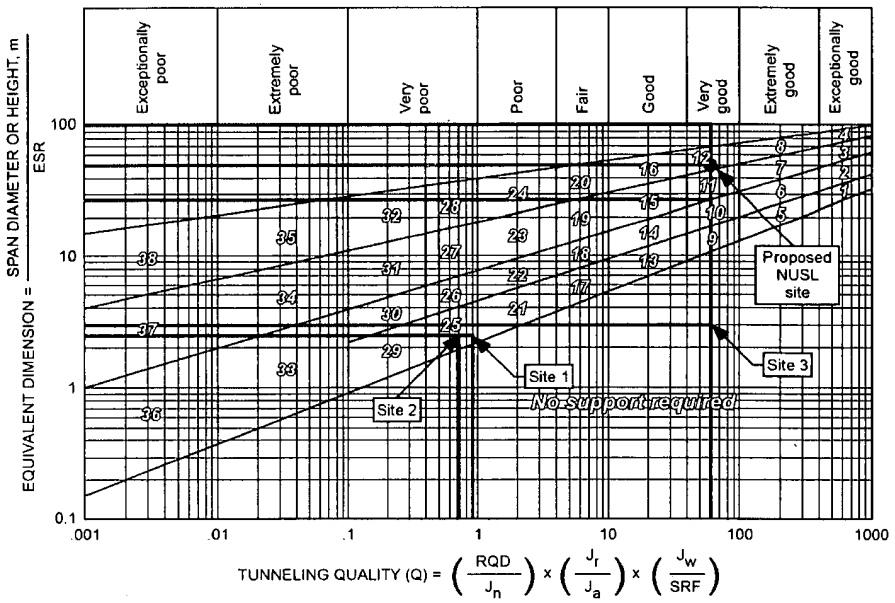

Figure 3.—Recommended support as a function of tunneling quality index and equivalent dimension (after [3])

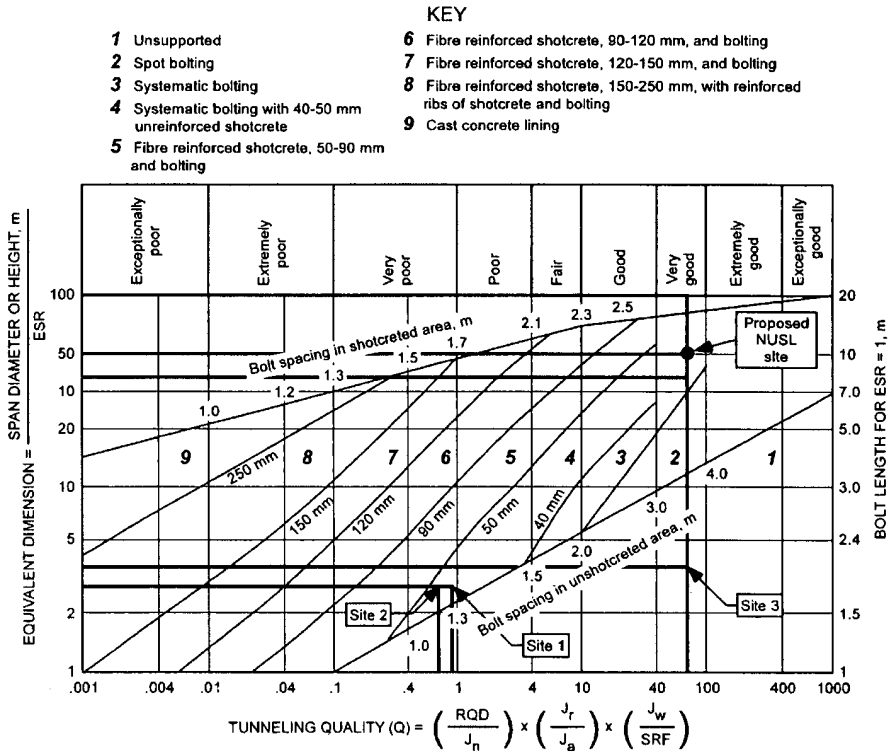

Figure 4.—Recommended support as a function of tunneling quality index and equivalent dimension (after [4])

Table 1.—Support recommendations based on Q compared to actual support used at three sites at the Homestake Mine.

Parameter	Site 1	Site 2	Site 3
Joints/m^3, J_v	16 (13 bedding planes + 3 joint sets)	12 (7 bedding planes + 5 joint sets)	<4
RQD = 115 - 3.3 J_v	60	75	85 (reduced from 100 for unknown joints)
Joint set number, J_N	3 (one joint set + random joints)	4 (2 joint sets)	0.75 (massive, no or few joints)
Joint roughness number, J_R	1 (smooth, planar)	1 (smooth, planar)	4 (discontinuous joints)
Joint alteration number, J_A	1 (unaltered joint walls)	1 (unaltered joint walls)	0.75 (tightly healed joints)
Joint water reduction number, J_w	1 (dry)	1 (dry)	1 (dry)
Stress reduction factor, SRF	20 (σ_c/σ_1[1] = 0.7)	20 (σ_c/σ_1 = 1.2)	10 (σ_c/σ_1 = 4.4)
Tunneling quality index, Q	1.0	0.9	60
Excavation support ratio	1.6 (permanent mine opening)	1.6 (permanent mine opening)	1.6 (permanent mine opening)
Span, m	4	4	5
Equivalent span, m	2.5	2.5	3.1
Recommended support [4]	Category 4 Rock bolts at 1.3-m spacing, 50-mm shotcrete	Category 4 Rock bolts at 1.3-m spacing, 50-mm shotcrete	No support required
Recommended support [3]	Category 25 Untensioned bolts at 1-m spacing, chain link mesh	Category 25 Untensioned bolts at 1-m spacing, chain link mesh	No support required
Actual support used	Friction bolts at 1-m spacing, chain link mesh	Friction bolts at 1-m spacing, chain link mesh	Spot bolting with mechanical-anchor bolts, friction bolts at 1.5-m spacing, chain link mesh

[1]σ_c = rock unconfined compressive strength. σ_1 = major principal stress.

Table 2.—Support recommendations for three roof spans where Q = 60.

Parameter	Span = 25 m (82 ft)	Span = 50 m (164 ft)	Span = 100 m (328 ft)
Excavation support ratio, ESR	1 (large civil cavern)	1 (large civil cavern)	1 (large civil cavern)
Equivalent span, m (ft)	25 (82)	25 (82)	100 m (328 ft)
Required support [4]	Category 4 Systematic bolting 40-50-mm shotcrete	Category 4 Systematic bolting 40-50-mm shotcrete	No recommendations
Required support [3]	Category 11 Tensioned bolts 2-3-m spacing	Category 12 Tensioned bolts 2-3-m spacing	No recommendations

5. CONCLUSIONS

The stability of a mine opening spanning 50 m with a volume of 163,624 m^3 was analyzed at depths from 2141 to 2416 m using the three-dimensional, finite-difference numerical model FLAC3D and empirical rock characterization techniques. Material properties and in situ stresses from a previously calibrated finite-element model applied to vertical crater retreat stopes in the Poorman and Homestake formations were used. The model calculated zones of plasticity around the mine opening at all mining depths below 2141 m. The maximum extent of failure into the rock was 10 m and would occur in the lower roof at all mining depths modeled. However, the thickness of the failure zone diminished to zero near the apex of the hemispherical roof. The maximum yield width in the room's rib was 6.8 m.

These results, combined with observations of instability of rooms by mine personnel at 2438 m underground, suggest that 2141 m may be the deepest level that a room spanning 50 m can be mined and maintained in rock with strengths equal to those of the Poorman and Homestake formations. If the rock strength obtained from the specimens of Yates Forma-

tion rock are representative of the entire formation, then construction of large rooms may be possible at levels below 2141 m in this host rock, but may raise rock bursting concerns. A thorough site investigation in the Yates Formation, including joint mapping and directional drilling to obtain core for laboratory tests, is essential for a more accurate stability assessment.

Rock support requirements were validated at three existing sites using empirical design methods, indicating that it is reasonable to apply these methods to the large chamber proposed at the Homestake Mine. The recommended spacing between bolts for a 50-m span constructed in rock believed to be characteristic of the Yates Formation is 2 to 3 m. A 50-mm-layer of shotcrete is also advised.

ACKNOWLEDGMENTS

The authors wish to express their appreciation to Mark Laurenti, chief mine engineer; Mike Stahl, mine production engineer; and Kathy Hart, chief geologist, Homestake Mining Co., for providing access to underground workings and providing historic stability information on large excavations at the Homestake Mine. Modeling suggestions made by John D. Osnes, manager of Geomechanics, RESPEC, Rapid City, SD, are also much appreciated.

REFERENCES

1. Davis, Rachel, ed. 2001. Underground lab to mine secrets of the universe. *Engineering Times*, Aug./Sep.

2. Itasca Consulting Group, Minneapolis, MN. 1998. FLAC - Fast Lagrangian analysis of continua, version 3.4. 1485 pp.

3. Barton, N.R., R. Lien, and J. Lunde. 1974. Engineering classification of rock masses for the design of tunnel support. *Rock Mech.* 6(4):189-239.

4. Grimstad, E., and N. Barton. 1993. Updating the Q-system for NMT. In *Proceedings of the International Symposium on Sprayed Concrete: Modern Use of Wet Mix Sprayed Concrete for Underground Support.* Oslo: Norwegian Concrete Assn.

5. Pariseau, William G. 1985. Research study on pillar design for vertical crater retreat (VCR) mining. Bureau of Mines Contract Report J0215043, Oct.

6. Pariseau, William, F. Duan, and C.S. Schmuck. 1987. Stability analysis of the VCR stope at the Homestake Mine. *Gold Mining 87,* pp. 199-213.

APPENDIX B

STOPE STABILITY AS A FUNCTION OF DEPTH AT THE HOMESTAKE MINE – PARISEAU, W. AND DUAN, F.

"Stope Stability as a Function of Depth
at the Homestake Mine"

By

Bill Pariseau and Fei Duan

Introduction

This memorandum summarizes a short series of finite element analyses of stope stability at the Homestake Mine in Lead, South Dakota. The purpose of the analyses was to determine the sensitivity of stope stability to changes in depth from 6,000 feet below surface to 9,000 feet. The in situ stress state, rock properties, and stope geometry are similar to those determined during a rock mechanics study of a stope between the 6950 and 7100 levels. The panels in this stope are mined by the vertical crater retreat method (VCR).

The analyses show a gradually increasing yield zone with increasing depth. There is no abrupt expansion of potential yield zones nor sudden change in stability with increasing depth from 6,000 to 9,000 feet. This conclusion is, of course, limited to the conditions used in the analyses.

In Situ Stress State

The in situ stress was calculated from the formulas developed in the rock mechanics study of the instrumented stope between the 6950 and 7100 levels. These are:

$$S_v = 1.25\ h \qquad \text{(vertical stress)}$$

$$S_{h1} = 2078 + 0.57\ h \qquad \text{(perpendicular to strike)}$$

$$S_{h2} = 121 + 0.53\ h \qquad \text{(parallel to strike)}$$

Where h is the depth below surface in feet and the stresses are in psi. Table 1 summarizes the in situ stresses at the four depths used in the present analysis series.

Table 1. In Situ Stresses at Different Depths

Depth below surface in (ft)*	Vertical stress S_v (psi)	Horizontal stress S_{h1} (psi)	Horizontal stress S_{h2} (psi)
6000	7,500	5,498	3,301
7000	8,750	6,068	3,831
8000	10,000	6,638	4,361
9000	11,250	7,208	4,891

*Measured to the stope bottom.

Stope Geometry

The stope is 50-ft wide measured horizontally across the vein from footwall to hanging wall as shown in Figure 0. Stope height measured vertically between levels is 150 feet; dip is 60°. These dimensions are representative of actual stope dimensions, although there is considerable variation.

Stope Geology

A three formation geological model was used in the analyses. The Poorman formation is in the footwall; the Ellison formation was assumed to constitute the hanging wall; and the Homestake formation is in between. The stope extends across the Homestake formation from footwall to hanging wall (as seen in Figures 1-5).

Rock Properties

The elastic moduli and strength used in the analyses are the same rock mass properties determined in the rock mechanics analysis of the study stope data. The three formations (Homestake, Poorman, and Ellison) are anisotropic (orthotropic) and require nine elastic moduli and nine strengths. These are given in Table 2. The subscripts 1, 2, 3 refer to directions perpendicular to the dip, down-dip, and parallel to strike, respectively.

Table 2. Anisotropic Rock Mass Properties for the Homestake Mine

Property Index*	Homestake Formation	Poorman Formation	Ellison Formation
E_1	4.59×10^6	4.68×10^6	4.86×10^6
E_2	3.35×10^6	3.30×10^6	2.59×10^6
E_3	3.24×10^6	3.96×10^6	4.93×10^6
V_{12}	0.14	0.20	0.23
V_{23}	0.18	0.17	0.15
V_{31}	0.19	0.15	0.22
G_{12}	1.73×10^6	1.66×10^6	1.38×10^6
G_{23}	1.40×10^6	1.52×10^6	1.42×10^6
G_{31}	1.55×10^6	1.85×10^6	2.01×10^6
C_1	16117	9073	10939
C_2	9237	1695	8000
C_3	10613	6524	9812
T_1	1103	1880	2396
T_2	911	471	656
T_3	1545	1320	1531
R_1	1640	920	1200
R_2	1975	1695	2237
R_3	1680	1000	1023

Note: All units are in psi except for Poisson's ratio.

*E = a Young's modulus, V = a Poisson's ratio, G = a shear modulus, C = a compressive strength (unconfined), T = a tensile strength, and R = a shear strength.

Results

The results of the finite element analyses are shown in Figures 1-4. These figures show safety factor contours and yield zone extent in the vicinity of the generic stope. The depth is measured from surface to haulage level (stope bottom). The data in Figures 1-4 are similar in the sense that yield zones extend from the sharp corners of the mined (and unfilled) stope. The hanging wall yield zone extends from the haulage level upwards; the footwall yield zone extends from the top sill downwards.

Although a footwall haulage drift is present, there is no cable bolt drift in the hanging wall in these analyses. If a cable bolt drift were present, its effect on the hanging wall would be similar to the effect that the haulage drift has on the footwall. This effect consists of a stress concentration about the drift and a concentration of stress between the drift and the stope. The results in Figures 1-5 show a localized yield zone in the ribs of the pillar between the footwall haulage drift and the stope footwall. A similar occurrence would be expected if a cable bolt drift was present in the hanging wall. The localized yield zones in the ribs do not link to form a zone of yielding across the entire footwall pillar even at the 9,000 ft depth. However, there is a potential for such linkage to occur. This suggests that the footwall haulage drift be located farther from the stoping area as depth increases. In this regard, yielding would be aggravated by blast damage accumulation, so observation of the footwall haulage drift ribs and crosscuts to the stope bottom sill would be in order at such depths. The same would be true if cable bolt drift were used in the hanging wall.

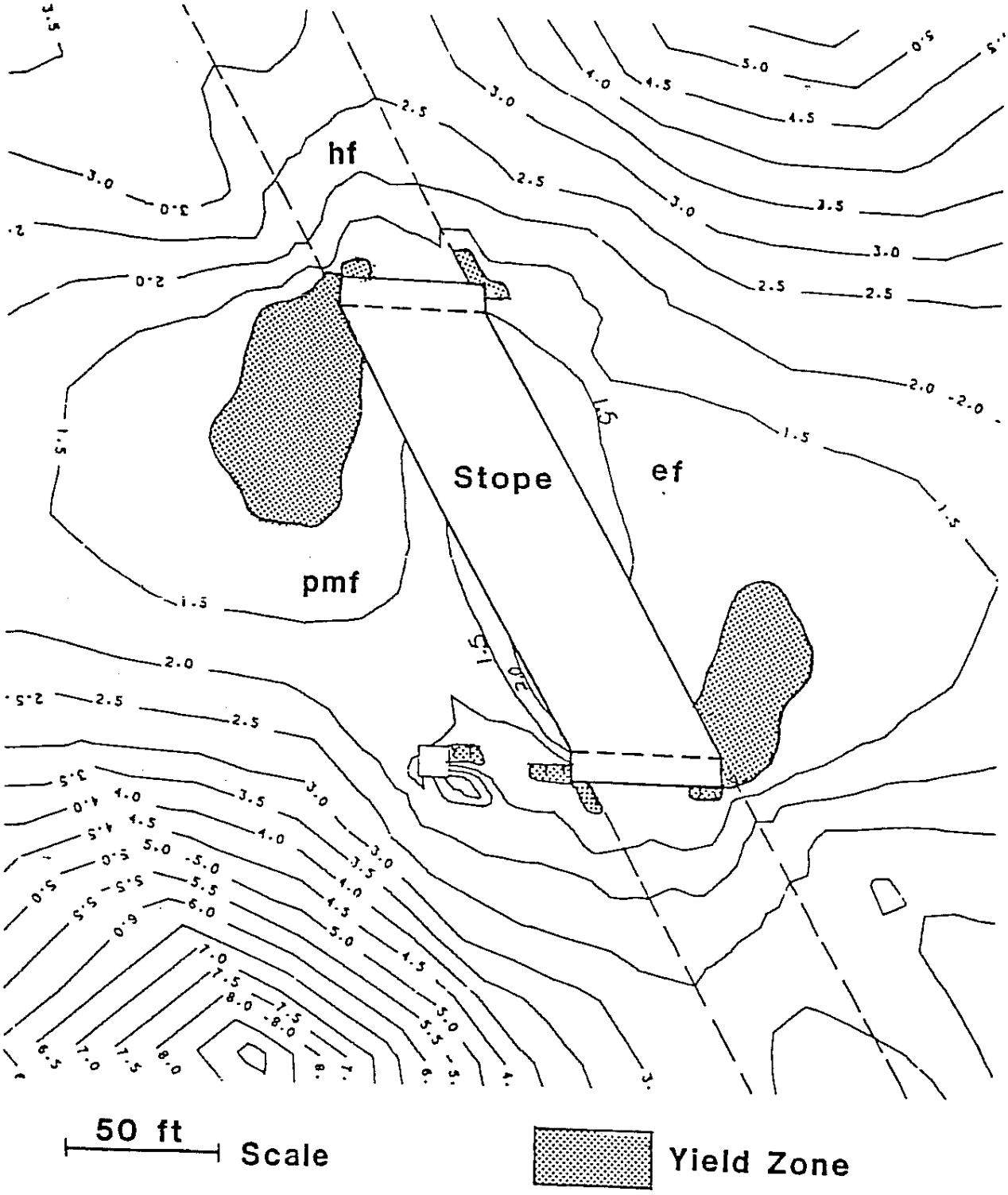

Figure 1. Safety Factor Contour at Depth = 6000 ft.

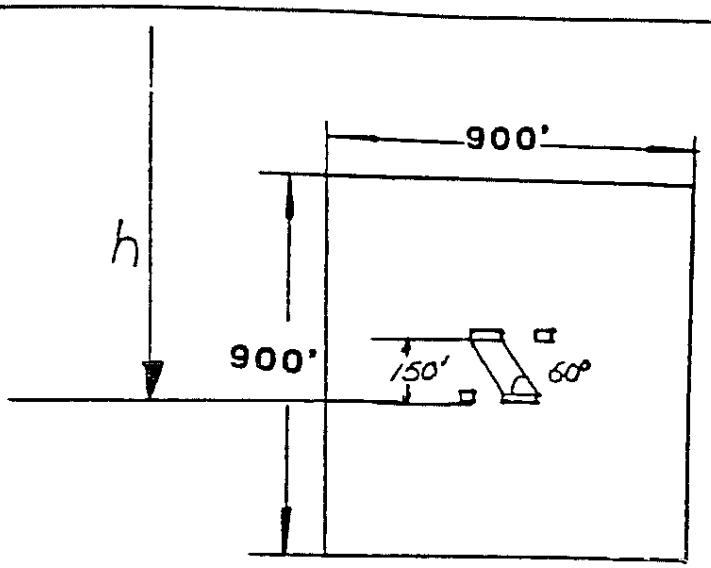

Figure 0. Stope Geometry and Overall Model Dimensions.

* The depth h is measured to the bottom of the stope (from the surface) as shown in Figure 0.

Conclusion

Analyses of a generic VCR stope at depths of 6,000 to 9,000 ft show a gradually increasing extent of potential yield zones with depth. The conditions of the analysis are similar to those developed from the study stope between the 6950 and 7100 level and are considered representative of actual conditions. There is no abrupt decrease in stability with depth; there is no sharply defined critical depth below which stability could not be achieved according to the results reported here. These results include the interaction between the stope and footwall haulage drift. No hanging wall cable bolt drift was present in the analysis. The results suggest that the footwall haulage drift may need to be located farther from the stope as depth is increased towards 9,000 feet.

The ground within a yield zone (shown as a shaded region in Figures 1-5) is at the elastic limit and thus has a safety factor of 1.0. Outside the yield zones, the local factor of safety is greater than 1.0. The contours in Figures 1-4 are contours of the local safety factor at intervals of 0.5. As depth increases from 6,000 to 9,000 ft, the analyses show an increasing amount of ground between the yield zones and the 1.5 contour. The 1.5 safety factor contour moves away from the stope as more ground becomes more highly stressed and the yield zones extend further from the sharp stope corners. This is as expected.

Figure 5 shows the yield zones at the four depths used in the analyses and indicates the growth of potential yield zones with increasing depth. The growth is gradual; there is no abrupt increase in yield zone extent with depth. There is, therefore, no abrupt change in stope stability with depth nor a sharply defined critical depth below which stope stability would be highly questionable while at shallower depths would not be a problem.

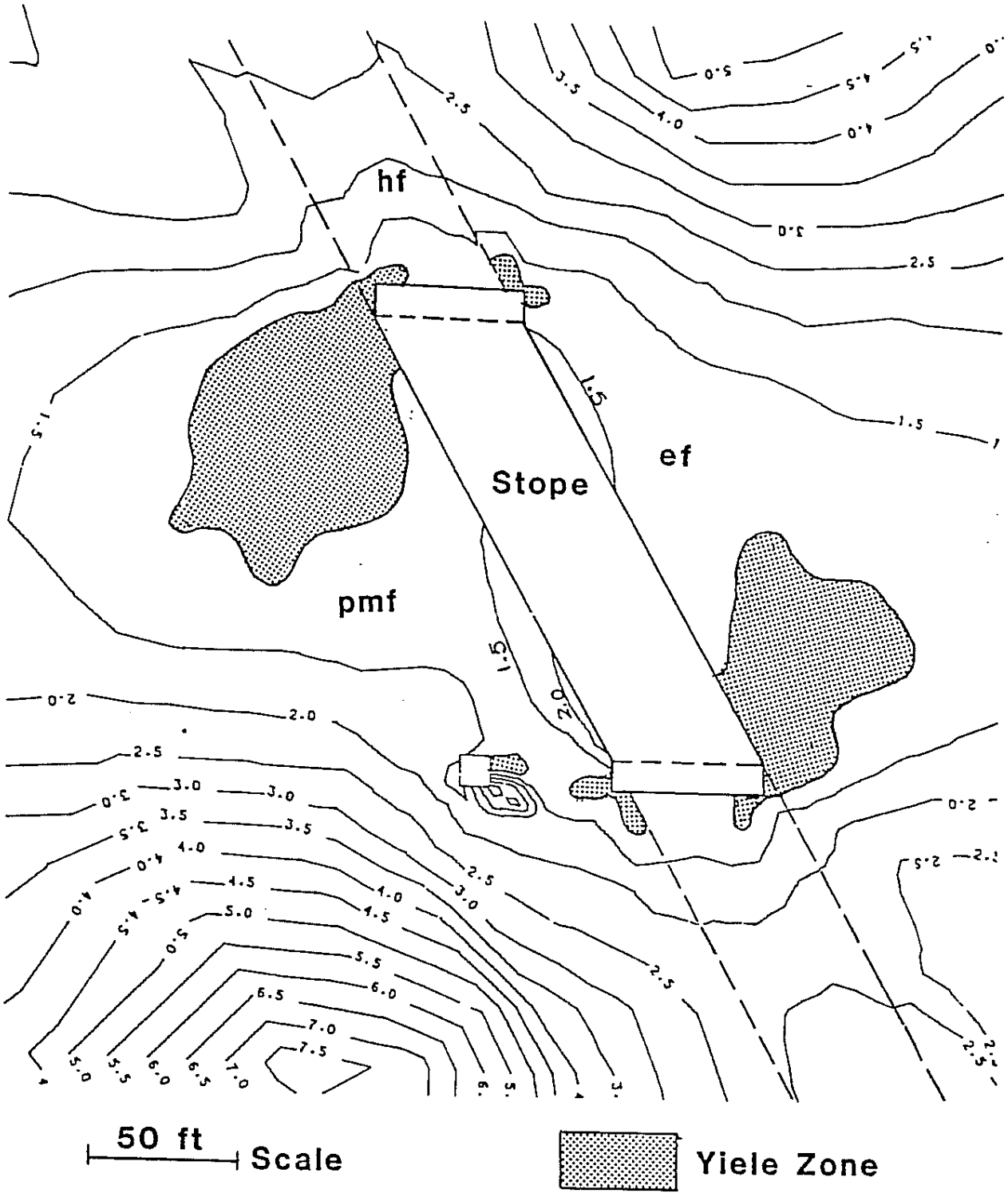

Figure 2. Safety Factor Contour at Depth = 7000 ft.

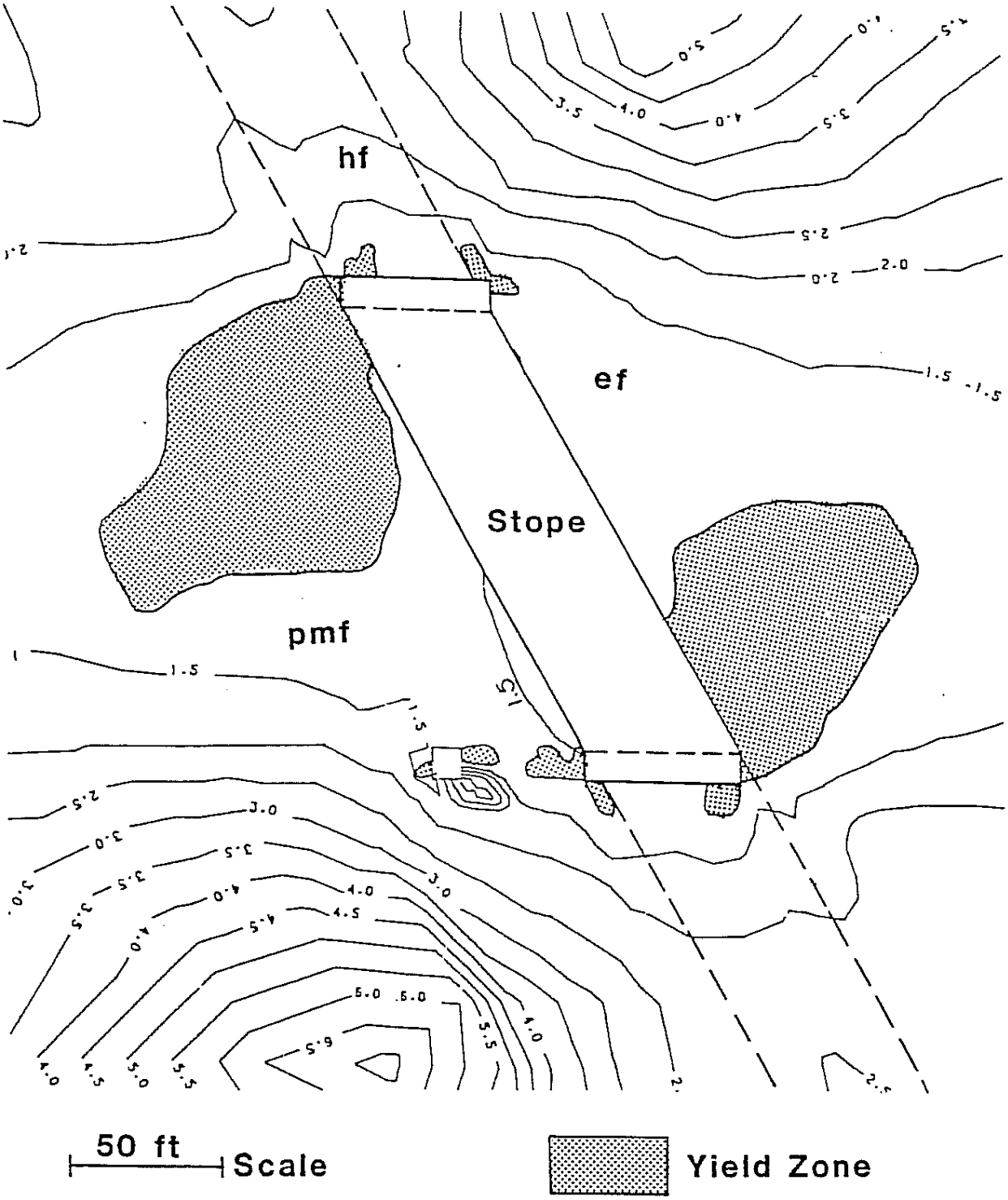

Figure 3. Safety Factor Contour at Depth = 8000 ft.

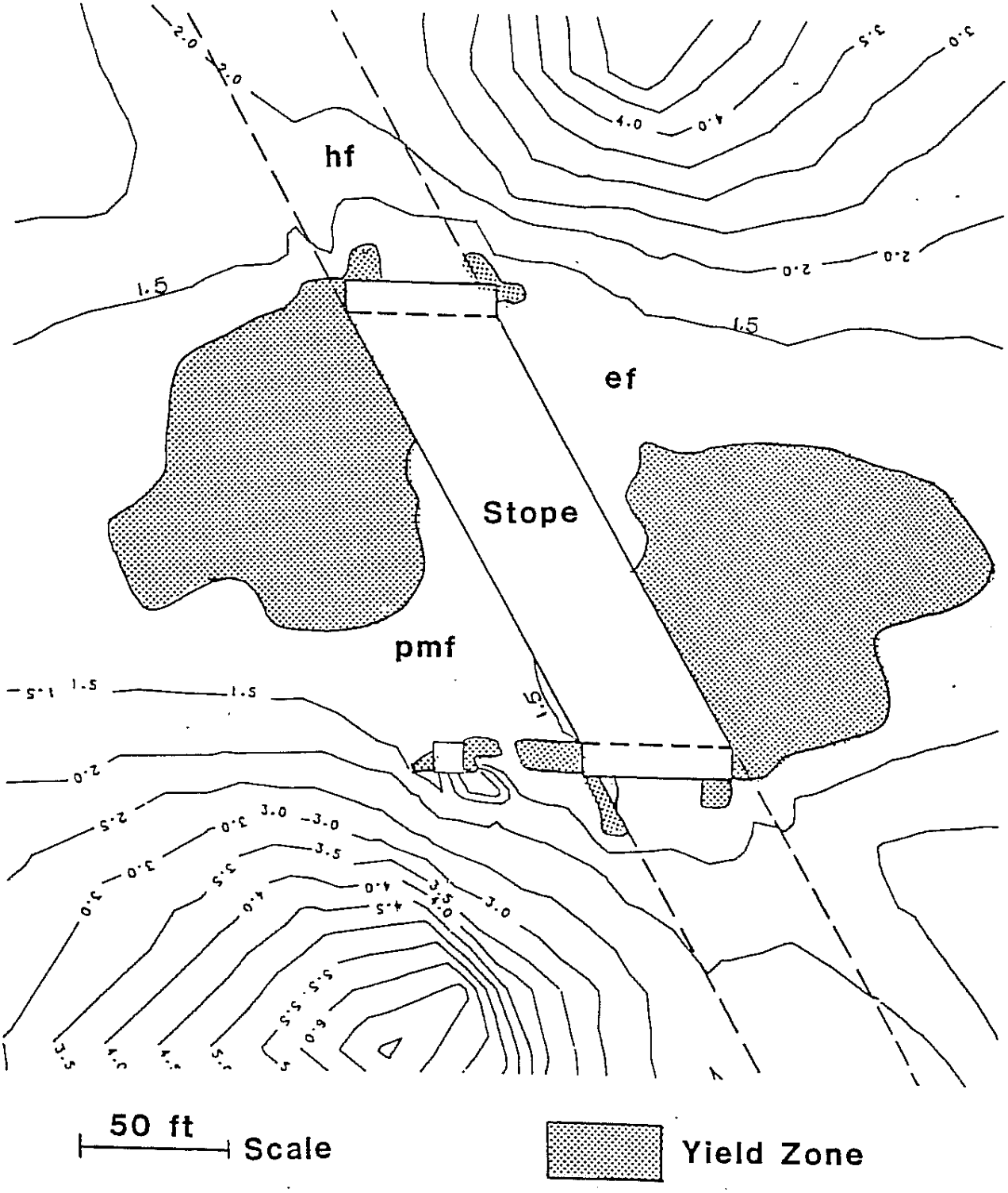

Figure 4. Safety Factor Contour at Depth = 9000 ft.

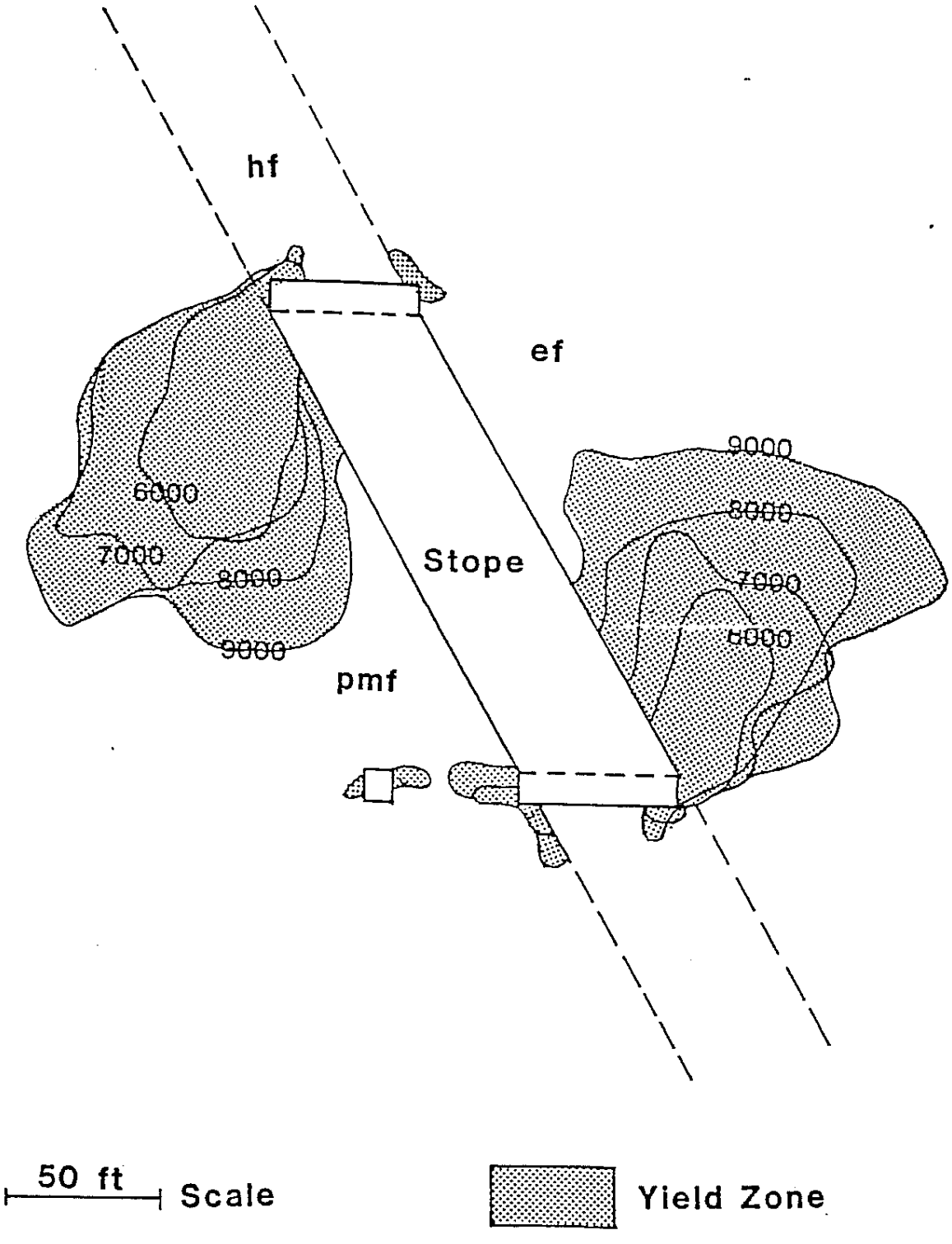

Figure 5. Yield Zone Growth With Depth.

APPENDIX C

DESTRESS BLASTING IN HARD ROCK MINES – A STATE OF THE ART REVIEW – MITRI, H.S. AND SAHARAN, M.R.

Rock Engineering

Destress blasting in hard rock mines—a state-of-the-art review

H.S. Mitri, McGill University, Montreal, Quebec, and
M.R. Saharan, Central Mining Research Institute, Nagpur, India

KEYWORDS: Rockburst, Rockburst control measures, Destress blasting, Ground control, Underground mining, Hard rock mines.

Paper reviewed and approved for publication by the Rock Engineering Society of CIM.

ABSTRACT

A brief overview of rockburst control measures is presented. The paper then elaborates on one key rockburst control measure, which is known as destress blasting. A historical background of the technique is presented in order to understand different aspects of its field application. The publication enumerates key aspects of the technique as being used in practice in South Africa and North America. The paper also presents an analysis of three case studies in order to demonstrate difficulties associated with the field application of destress blasting in hard rock mines.

Brief Overview of Rockbursts and Their Control Measures

The mining industry has been dealing with rockburst problems since they were first reported in a gold mine in India at the end of the 19th century (Morrison, 1942; Blake, 1972a). Since then, there has been a worldwide increase in the reported incidences of rockbursts as mining operations reached deeper ore deposits with higher ore extraction ratios, thus leaving behind less pillar support. Intensive research has been carried out to identify the root causes of rockburst and to develop means of controlling or even alleviating rockburst hazards. These studies resulted in a better understanding of brittle rock failure characteristics as well as the formulation and implementation of energy theories. For example, Salamon (1970, 1974) presented a detailed review of the energy balance concepts and introduced the concept of the energy release rate (ERR). More recently, Mitri et al. (1999) introduced the concept of the energy storage rate (ESR). Such studies led to a better understanding of the different types of strainbursts and their causes. Figure 1 presents rockburst classification as proposed by Brown (1984) and later accepted by the Canada Rockburst Research Program (CRRP, 1996). While much has been learnt about rockbursts, their prediction is still a mystery. Contributory factors to strainbursts such as high stresses, stiff rock strata, rapid mining cycles, and larger excavation areas are known but their triggering mechanism and likelihood of triggering time cannot be predicted. Therefore, much attention has been and is still being paid to the development of rockburst control and containment measures.

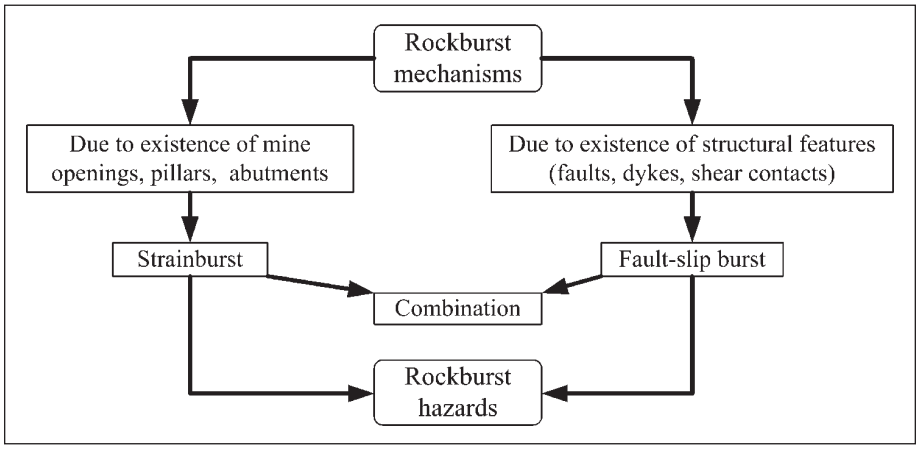

Fig. 1. Classification of rockburst mechanisms (adapted from CRRP, 1996).

Figure 2 depicts the various rockburst control measures (Mitri, 2000). The application of alternative mining methods was the first reaction in response to the increasing rockburst incidences in the early part of the 20th century. Initial observation of rockbursts led to the conclusion that pillar formation during mining operations is prone to rockbursts. Hence, pillarless mining, such as the longwall mining method, was introduced and implemented (Anon, 1939). Pillars are, however, unavoidable in many mining situations. The yield pillar technique in conjunction with sequential mining was applied to continuously dissipate the energy from overlying strata (Salamon, 1970). Mining with a protective seam provided much relief from rockbursts, whenever such a seam (with uneconomical mineral value) was present and excavated prior to the excavation of the main seam (Staroseltsev and Sysolyatin, 1979). Further, observations bring out the point that alternative mining methods were attempted as a means of combating rockburst hazards. For example, Board and Fairhurst (1983) reported a preference for the change of mining method from overhand cut-and-fill to underhand cut-and-fill. Also, Williams and Cuvellier (1988) reported that the mines in the Coeur d'Alene Mining District, Idaho, switched to the underhand longwall mining method before closing due to economical reasons.

The trend towards providing more support to the rock mass to control rockburst events received equally strong attention. It was thought that if an excavated area can be back-

Hani Mitri
is a professor of mining engineering in the Department of Mining, Metals and Materials Engineering at McGill University. Since he joined the department in 1986, he established the Mine Design and Numerical Modeling Laboratory and the Rockbolting Instrumentation Laboratory. His current research activities relate mainly to rock mechanics and rock supports, ore dilution, dynamic stability of tailings dams, and road foundations with geosynthetics. He is a registered professional engineer in Quebec and a member of several national and international committees.

Mani Ram Saharan
is a mining engineer and scientist with the Central Mining Research Institute of India (CMRI). Since he joined CMRI in 1996, he has been involved in a number of research projects related to underground mining and rock mechanics. He obtained his Ph.D. degree in mining engineering from McGill University in May 2004. He was awarded the Dean's Honor List for his thesis.

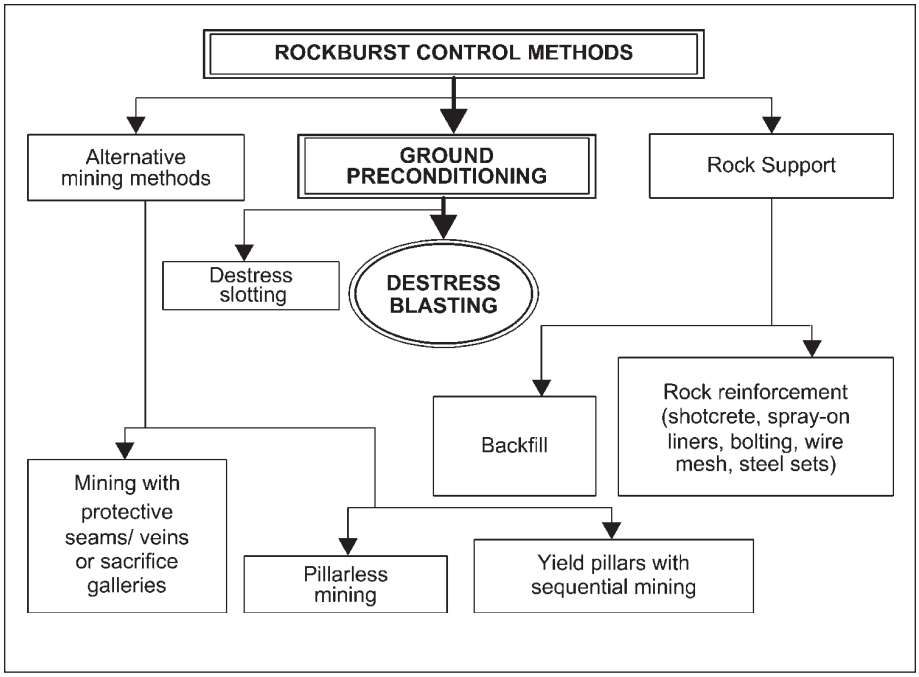

Fig. 2. Rockburst control methods (adapted from Mitri, 2000): a) face perpendicular pre-conditioning, b) face parallel pre-conditioning.

filled then it would prevent strata movement and hence would reduce rockbursts. Backfills were also considered as a cushioning medium to reduce the burst impact effect. It was realized, however, that backfills are not very effective in reducing rockburst occurrence though the severity could be limited (Wiggill, 1963). Rock reinforcement was adopted with the consideration that rock reinforcement should have yielding characteristics (Kaiser, 1993). This concept stems from structural engineering, whereby earthquake-resistant structural elements are designed to have large energy-absorption capacity. Therefore, rock reinforcement made from ductile support elements are preferred. So far, however, the applicability of rock reinforcement measures to contain rockbursts has not yet been fully proven. This can be attributed to the difficulty of estimating the magnitude of a rockburst event for a given mining situation.

Pre-conditioning, which is another important rockburst control measure (Fig. 2), has been used to control strainbursts since the beginning of the 20th century (McInnes et al., 1959). The practice of destress slotting and destress blasting has proved successful in controlling rockburst hazards in coal mines (Brauner, 1994). While both destressing techniques are used in hard rock mines, destress blasting is by far more popular.

Historical Background of Destress Blasting

A common notion has permeated that destress blasting was conceived and first applied in the gold mines of South Africa (Roux et al., 1957). Contrary to this belief, literature indicates that Springhill Colliery, Nova Scotia, Canada (McInnes et al., 1959) introduced and applied destress blasting as a rockburst control measure in the early 1930s. Christian (1939) reported the first application of destress blasting for hard rock mines in Teck-Hughes Mines, Canada. The mines of Kirkland Lake, Ontario, Canada, used destress blasting in the 1930s on a trial and error basis (Hanson et al., 1987).

The first set of systematic observations of destress blasting and its benefits, however, are documented with the detailed experiments conducted in the early 1950s in gold mines of the Witswatersrand area, South Africa (Hill and Plewman, 1957; Roux et al., 1957; Gay et al., 1984). The concept of destress blasting evolved from the field observation that the zone of highly fractured rock immediately surrounding some deep underground openings seems to offer some shielding to both the occurrence of and damage from rockbursts. It was argued that extending and maintaining this zone of the fractured rock ahead of a face can reduce both the occurrence and the effects of rockbursts. Effectiveness of the concept was tested in the field and involved destress blasting of 32 stopes over a 19-month period at the East Rand Proprietary Mines Ltd. The results were encouraging. The incidence of rockbursts, severity of rockbursts, time of rockbursts (relative to shifts), and causalities were among the parameters monitored before and after destress blasting. Improvements ranged from 34% reduction in rockbursts incidence to 100% elimination of casualties (Roux et al., 1957).

Destress blasting was again re-evaluated for South African gold mines in the late 1980s (Brummer and Rorke, 1988; Rorke et al. 1990; Adams et al., 1981, 1993; Lightfoot et al., 1996; Toper et al., 1997). Figure 3 illustrates two of the commonly practiced destress blasting schemes in South African gold reefs: face perpendicular and face parallel destressing schemes (Toper et al., 1997). As can be seen from the schematic plan view in Figure 3a, face perpendicular destressing (or preconditioning) uses evenly spaced blastholes (maximum spacing of 4 m) drilled perpendicular to the stope face in the plane of the gold reef and at mid-face height. The holes are drilled to a depth of 3m for an estimated face advance of 1 m/d; they are offset from the holes of the previous day by 50 cm, and are fired as an integral part of the production blast. The face-parallel pre-conditioning technique (Fig. 3b) involves drilling and blasting an 89 mm hole, which is 3.5 m to 5.5 m ahead of a mining face (panel) that is no more than 20 m long. The hole is drilled from a lead panel with a dedicated percussion drill, thus requiring that the mining face be divided into panels as shown.

The current practice has many notable departures from the original concepts of destress blasting. The following is a summary of the beliefs based on the references cited above associated with the current practice adopted after the re-evaluation of destress blasting:

- The main objective of destress blasting is to activate already existing tightly closed fractures rather than to initiate and propagate new ones.
- The position and depth of destress blastholes should be confined to the already fractured zone for an effective application.
- The aim of destress blasting is to shift stress concentrations and associated seismic activities deeper into the rock. The extent of the already fractured zone is generally 3 m to 5 m from the active face. Therefore, destress blasting should be part of a regular production cycle to be effective in continuously transferring seismic activities away from the face in a systematic manner.
- A low shock and high gas energy explosive (ANFO types) has a better effect in the opening and extending pre-existing fractures, and hence should be employed.
- Destress boreholes should be equally far from both the hangingwall and the footwall to keep them free of blast-induced damage and to minimize associated ground control problems. The borehole spacing of 3.0 m is established for the 38 mm diameter boreholes based on experience, borehole endoscopy, and ground penetrating radar.

In North American mines, destressing is more widely practiced (Dickhout, 1962; Moruzi

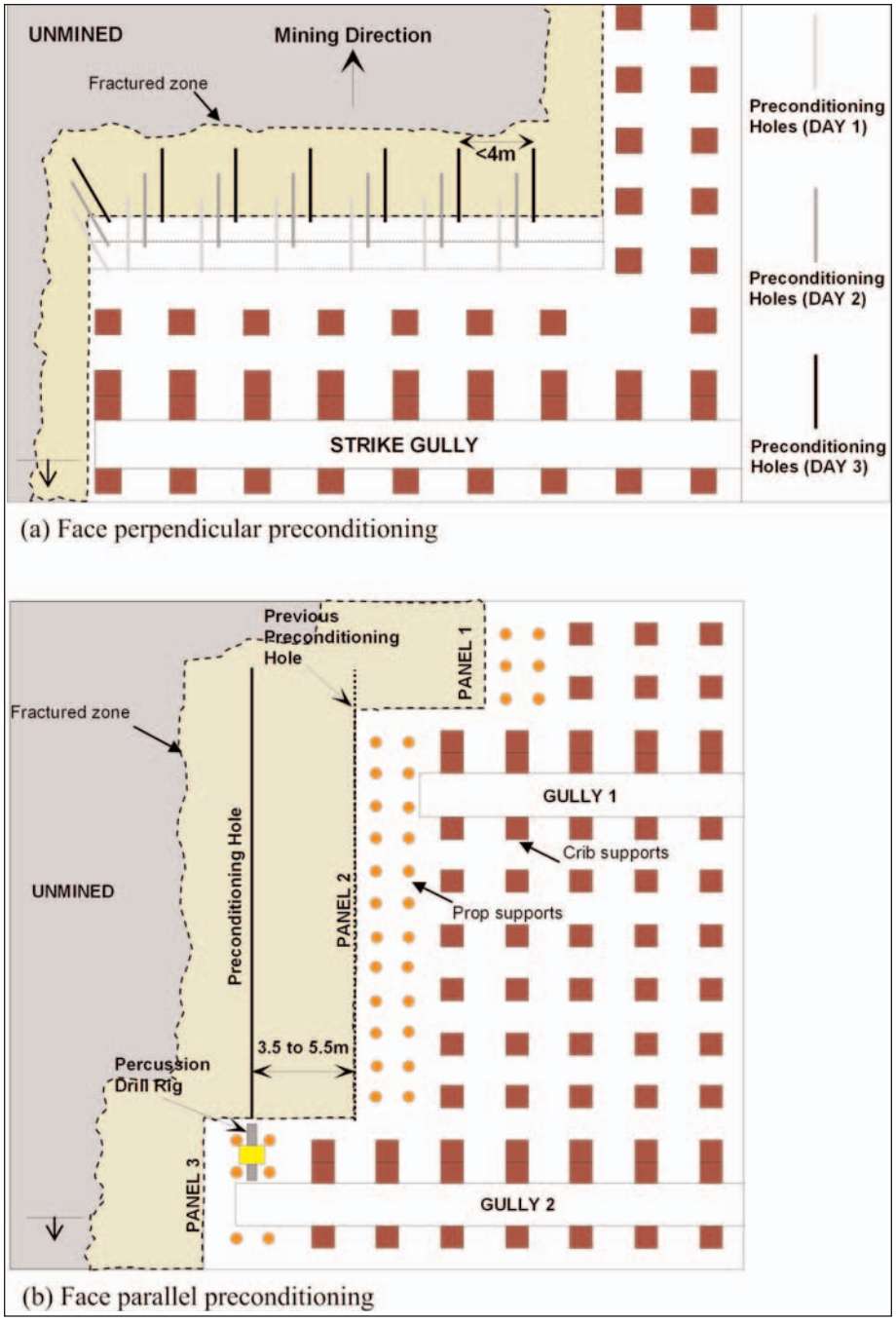

Fig. 3. Destress blasting practice in the gold mines of South Africa (adapted from Adams et al., 1993; Lightfoot et al., 1996; Toper et al., 1997).

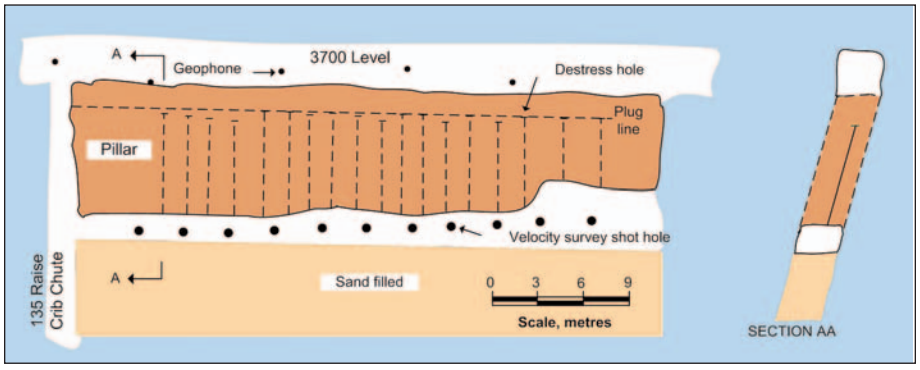

Fig. 4. Crown pillar destressing at the Galena mine (adapted from Blake, 1972b).

and Pasieka, 1969; Hedley, 1992; Mitri, 2000). Sill pillar destressing was done on a regular basis in the Coeur d'Alene mining district of northern Idaho. Several publications reported instrumented field trials for these mines (Blake, 1972a, 1972b; Corp, 1981; Board and Fairhurst, 1983). It was reported that destressing significantly reduces seismic activity during mining (Blake, 1982). Cooperative efforts by the United States Bureau of Mines and the mining companies showed that destress blasting could be effective for better rockburst control. Figure 4 illustrates a commonly adopted scheme of destress blasting in cut-and-fill mining whereby evenly spaced blastholes are drilled in crown pillar in the plane of the orebody. At the Galena mine, the crown pillar of the sand-filled stope under the 3700 level was destressed with this scheme while a microseismic system was installed at the level to monitor the stope seismicity before and after destressing.

Destressing is normally practiced in crown-and-sill pillars in thin, steeply dipping orebodies in Canadian mines such as those at Campbell Red Lake mine, Dickenson mine (now Red Lake mine), Falconbridge mine (Moruzi and Pasieka, 1969), and Kirkland Lake (Cook and Bruce, 1983; Hanson et al., 1987). Labrie et al. (1997) and Mitri (1996) also report the results of experimental and numerical studies of destress blasting on a sill pillar at the Sigma mine, Quebec. Destress blasting is in regular use at Inco's Creighton mine in mine development work and in pillars, which is a form of pre-conditioning (Oliver et al., 1987; MacDonald, et al., 1988; O'Donnell, 1992). The most recent application of destress blasting is reported from Brunswick mine, Canada (Liu et al., 2003; Andrieux et al., 2003).

The following summarizes the prevalent notions for destress blasting particularly applied to pillars and stopes of the steeply dipping veins of metal mines in North America.

- The main objective of destress blasting is to fracture highly stressed stiff rocks. The resultant effect of such exercises is to transfer mining-induced stresses away from the working areas of the mine. Destressing involves a change in rock mass properties (Blake, 1972a; Mitri et al., 1988) as well as a reduction in stresses after destress blasting (Tang and Mitri, 2001).
- The borehole depth is a function of the desired destressing area, the magnitude of the mining-induced stresses, the mining method, and the available mechanization in the mine. Boreholes of 9 m to 10 m depth for crown-and-sill pillars have been reported (Blake, 1972b). A higher magnitude of the induced stresses may necessitate destressing for the whole stope in advance with 20 m to 25 m deep boreholes

(Karwoski et al., 1979; Andrieux et al., 2003).

- The aim of destress blasting is to fracture overly stiff homogenous rock mass. Although powder factors as low as 0.2 kg/m^3 were used in vein mines (Mitri, 2000), explosive energy levels near to production blasting have been used (Brummer and Andrieux, 2002).
- Emulsion-type explosives as well as ANFO-type explosives are equally used (Willan et al., 1985).

There are reports of mixed successes of destress blasting due to ground control problems caused by it although it is considered one of the best techniques of controlling rockbursts (Blake, 1982; Roux et al., 1957; Oliver et al., 1987; Williams and Cuvellier, 1988; etc.). Corp (1981) reported that destress blasting was experimented in the walls instead of the vein to avoid the ground control problems in the silver producing mines of the Coeur d'Alene mining district, Idaho. Blake (1998) reported abandoning a portion of stope in this mining district, whereas Board and Fairhurst (1983) and Williams and Cuvellier (1988) reported a preference of changing mining methods over destress blasting.

While depth, stress, and rock conditions in many deep mines are conducive to severe bursting on a routine basis, experience has shown that bursting is infrequent and associated with particular geometries and geological structures. It shows that a considerable amount of natural self-destressing often accompanies mining activities (Roux et al., 1957; Corp, 1981). Destress blasting is mostly applied as a last resort, i.e. when the natural or self-destressing of strainburst prone structures cannot be induced by the design of the mining geometry and mining sequence (Blake, 1998).

Review of Three Case Studies

The effectiveness of destress blasting to fracture confined rock masses has remained doubtful. Scoble et al. (1987) used borehole endoscopy measurements at Campbell Red Lake mine; they reported that destress blasting contributed only to the extension of pre-existing fractures at a short distance of 1.4 m from 45 mm diameter boreholes. Labrie et al. (1997) reported an increase in the modulus of elasticity in the order of 11% after an experimental in situ destress blast at the Sigma mine. This adds complexity to the problem, as the post blast rock mass stiffness should be weaker than before the blast. Three case studies are presented in order to illustrate the complexities associated with destress blasting and its application in the field.

Case Study 1—Strathcona Mine, Falconbridge, Canada (Hanson et al., 1992)

Mining method: Cut-and-fill
Problem: Sill pillars rockbursting at cross-cuts and stoping area in the footwall. Stress fractures were observed in the backs and walls to a depth of 1.2 m, with fracturing more pronounced near the footwall contact. Destressing was attempted, based on the numerical modelling results, in areas considered to be critically overstressed after re-supporting such critical areas with 2.4 m bolts and wire-mesh (areas A, B, and D shown in the plan view of Figure 5). Destress blastholes were 5.5 m long.
Properties:
Rock—Good-quality feldspathic gneiss (Q= 25, RMR=73, UCS=300 MPa, E=40 GPa, m=10, s=0.05). Three joint sets with the predominant joint set, having 2 m to 4 m spacing and 3 m to 10 m in persistence, has rough undulating surface infilled with chlorite talc, which is a product of joint alteration.
Ore—Nickel sulphide (UCS=110 MPa, E=55 GPa)
Mining induced stresses—In excess of 100 MPa near the footwall contact as estimated by numerical modeling.
Destress blasting parameters: 5.5 m long, 63 mm diameter, 66 holes in 2.1 m burden and spacing, and 1.2 m stemming were fired with Magnafrac3000 explosives (emulsion) in footwall drift sidewalls (Fig. 5). Powder factor ranged from 0.11 to 0.16 kg/m^3.
Destress blasting result: The destress blast caused displacement of skin rock to a depth of 0.5 m in the line of blastholes along with wire mesh and necking of bolt plates. Craters 0.3 m deep were also formed at some places. Seismic activity of 2.7 on the Nuttli scale was observed by microseismic as well as regional seismic observations.
Review: The problem of rock bursting centered in the region of a larger stoping area in the footwall and an area that falls in between the excavation zones. Destress blasting triggered a rockburst of 2.7 on the Nuttli scale and also caused support damage. It appears that the place of destressing was in stress relaxation zones formed in the sidewalls based on the assumption of regional stress pattern in North America (high horizontal stresses as the major principal stress, which are perpendicular to the veins). Hanson et al. (1992) reported that seismic activities coincided with the destress blasts of the footwall and were centred in the low safety factor zones. These observations served as indicators of a successful destressing experiment.

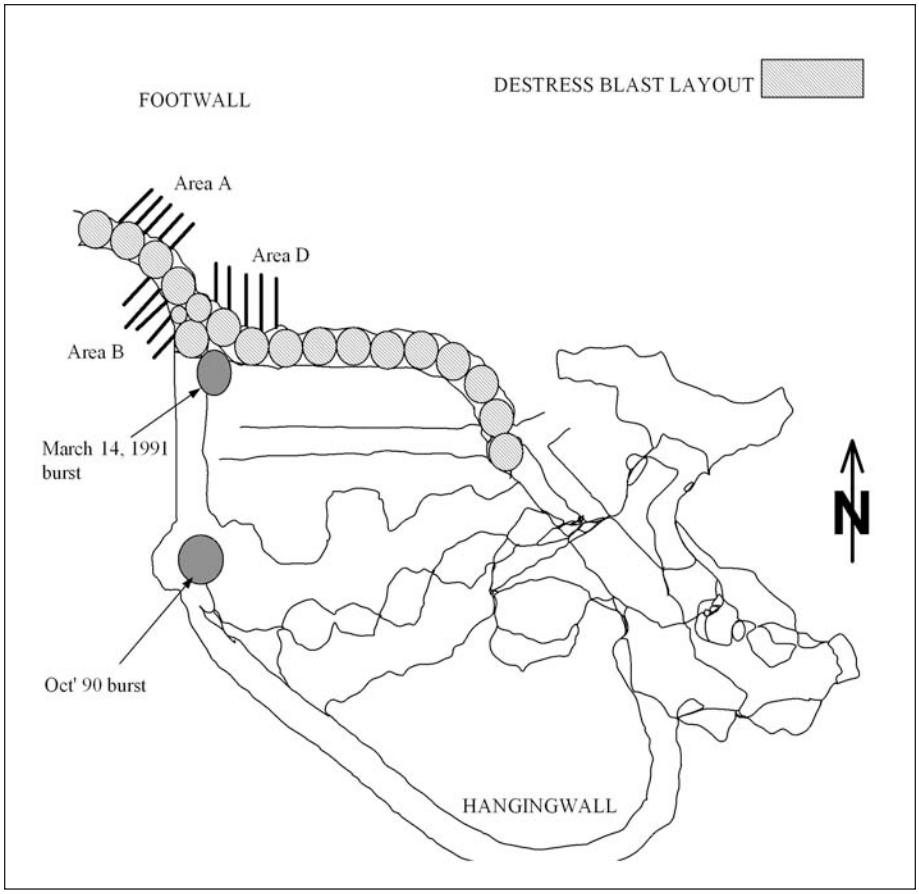

Fig. 5. Destress blasting in the drift at the Strathcona mine (adapted from Hanson et al., 1992).

Case Study 2—Star Mine, Coeur d'Alene Mining District, Idaho, United States (Karwoski et al., 1979; Corp, 1981; Blake, 1982)

Mining district: Half the silver and a majority of lead and zinc production for the United States are extracted from the mining district of Idaho where the mining depth is more than 2000 m. Ground control became a major issue because of the mining depth, major faulting and folding, and the hardness and brittleness of the rock mass. As a result of these problems, the Coeur d'Alene district has become one of the most extensively studied mining areas in the world.

Mining method: Cut-and-fill

Mining depth: Approximately 2400 m (7800 ft)

Problem: Below 2000 m depth, all the stopes were prone to bursting, regardless of the pillar size (resulting from cut-and-fill mining).

Ground conditions: Vertical stress is comparable with what might be expected from gravity loading. The horizontal stress, however, often exceeds the vertical (1.5 times at 2000 m depth). Estimated tensile strength of rocks varies from 8.3 to 26 MPa, UCS from 85 to 289 MPa, and the modulus of elasticity, E, ranges from 13.8 to 69 GPa. The wall rocks are a series of thin-and-thick, bedded quartzite with argillaceous interbeds.

Destress blasting parameters: Two in-vein ore blocks that are 76 m long by 12.5 m above and 12.5 m below the 7700 level by 1.5 m wide were drilled with a fan-shaped pattern up to 30 m long as shown in Figure 6. The destress holes were of 92 mm and 100 mm diameter. A total of 66 holes, 33 in each block, were drilled. The calculated powder factor is 0.28 kg/m^3. At the 7900 level, fan-shaped holes were drilled in 140 m strike length and 15 m above and below the level. Holes were loaded with emulsion-type explosives (Tovex 5000) with a charge density of 0.22 kg/m^3.

Destress blasting results review: The schematic of Figure 7 illustrates the stope extraction sequence (1 to 4) and the locations of the destressing experiments conducted. Reduced seismic velocity values in the vein and the walls subsequent to destress blasting at the 7700 level implied that reduced rock mass stiffness has prevented high-stress build-up. As mining progressed beyond the pre-conditioned zone, the release of seismic energy increased and rock bursting occurred. Some 20 incidences of bursts were observed. Closure measurements showed reduced stope closure, indicating a stiffer, more burst-prone vein and wall rock. Microseismic data showed that seismic activity in the non-preconditioned rock lasts longer after a stope production blast. All stopes in the vicinity were extracted without any significant seismic activity, possi-

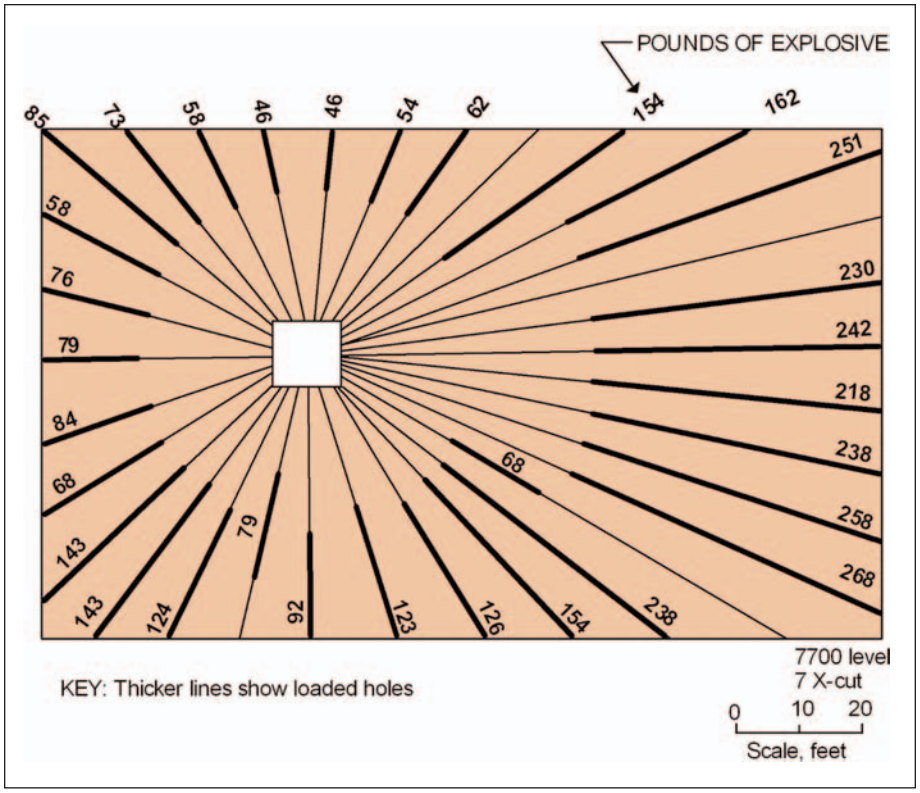

Fig. 6. In-vein destressing hole pattern at the Star mine around level 7700 (adapted from Karwoski et al., 1979).

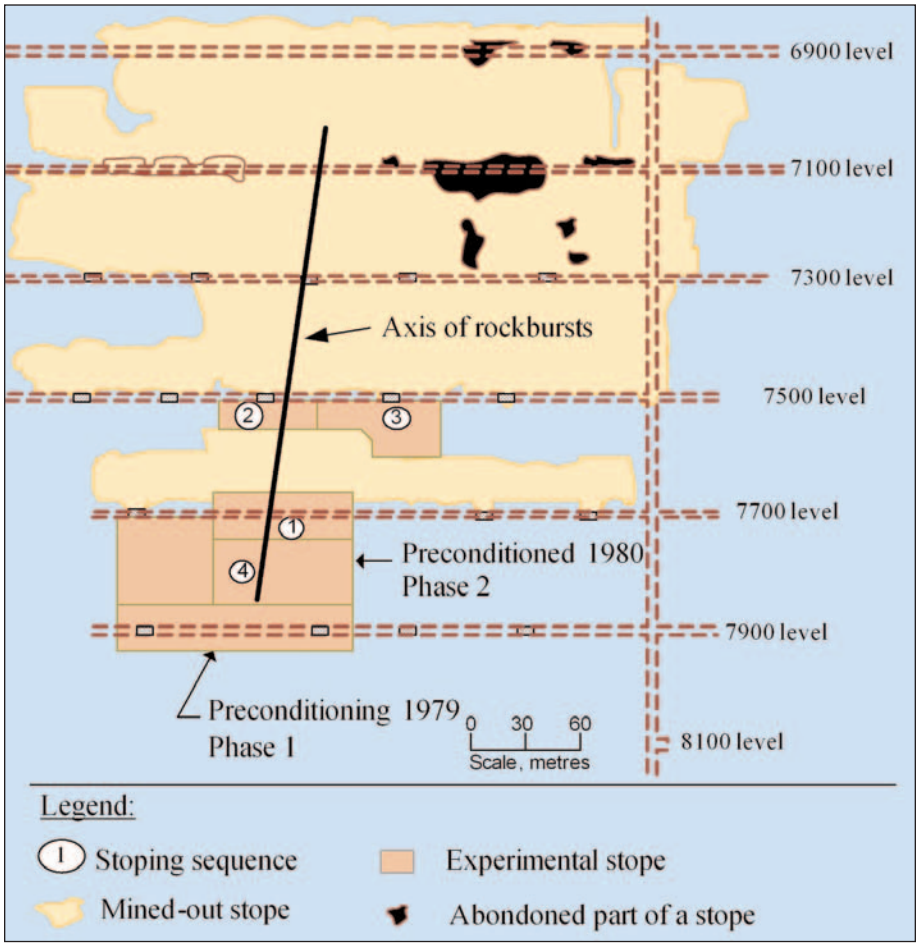

Fig. 7. Locations of experimental stope and pillar destressing at the Star mine (adapted from Blake, 1982): a) longitudinal section showing pillar 29-9, b) destress blasting pattern and instrumentation of the 29-9 pillar.

bly due to the destressing at the 7900 level. Stress transfer due to destressing, however, caused a rockburst of 2.6 M_L on the Richter scale below the 7500 level (stoping sequence 3 on Fig. 7). The majority of rockbursts occurred in the mine along the axis shown in Figure 7.

Case Study 3—Brunswick Mine, Canada (Andrieux et al., 2003; Liu et al., 2003)

Mining method: Open stoping with delayed backfill
Mining depth: 300 m at the 1000 level
Problem: Difficult mining due to high stresses. The particular pillar of the case study, 29-9, shown in Figure 8a, is made of strong and stiff low-grade sulphides. The purpose of pillar destressing is to create a stress shadow to facilitate the mining of two other parallel vein pillars containing high-grade ore.

Ore properties: Massive stiff sulphides (UCS=200 MPa, E=70 GPa, r =4.3 t/m^3)
Destress blasting parameters: 165 mm diameter blastholes with an average charge length of 20 m were at a 2.4 m by 2.4 m grid at the toe (Fig. 8b). Emulsion explosives with a total of 17,100 kg was used with no free face available to any of the holes. The powder factor is approximately 2.5 kg/m^3 for the 30 m high by 45 m long by 5 m wide block of the targeted 29-9 pillar.
Destress blasting result: The access drift from which destress blastholes were drilled showed that the drift closure was due to the material ejection after the destress blast. It may be worth noting that in addition to the normal confinement by rock mass, an additional confinement was provided to the destress blastholes by a pastefill spread in the drift.
Review: The study involves the extensive use of an array of sophisticated instruments and techniques such as borehole camera, a network of geophones, stress cells, multi-point borehole extensometers, etc. The results obtained from stress cells did not reflect the expected response due to concurrent mining in the adjacent stopes. It is not clear why the stress cell in the upholes showed stress relaxation while mining in the adjacent stopes should have resulted in stress build-up. The results obtained from the analysis of data, from borehole endoscopy and seismic tomography, indicate that the blasted pillar did not induce effective fracturing in the rockmass. Figure 9 shows the results of seismic tomography before and after the destress blast in terms of per cent change. As can be seen, there is no appreciable change in P-wave velocity around the destress-blasted column.

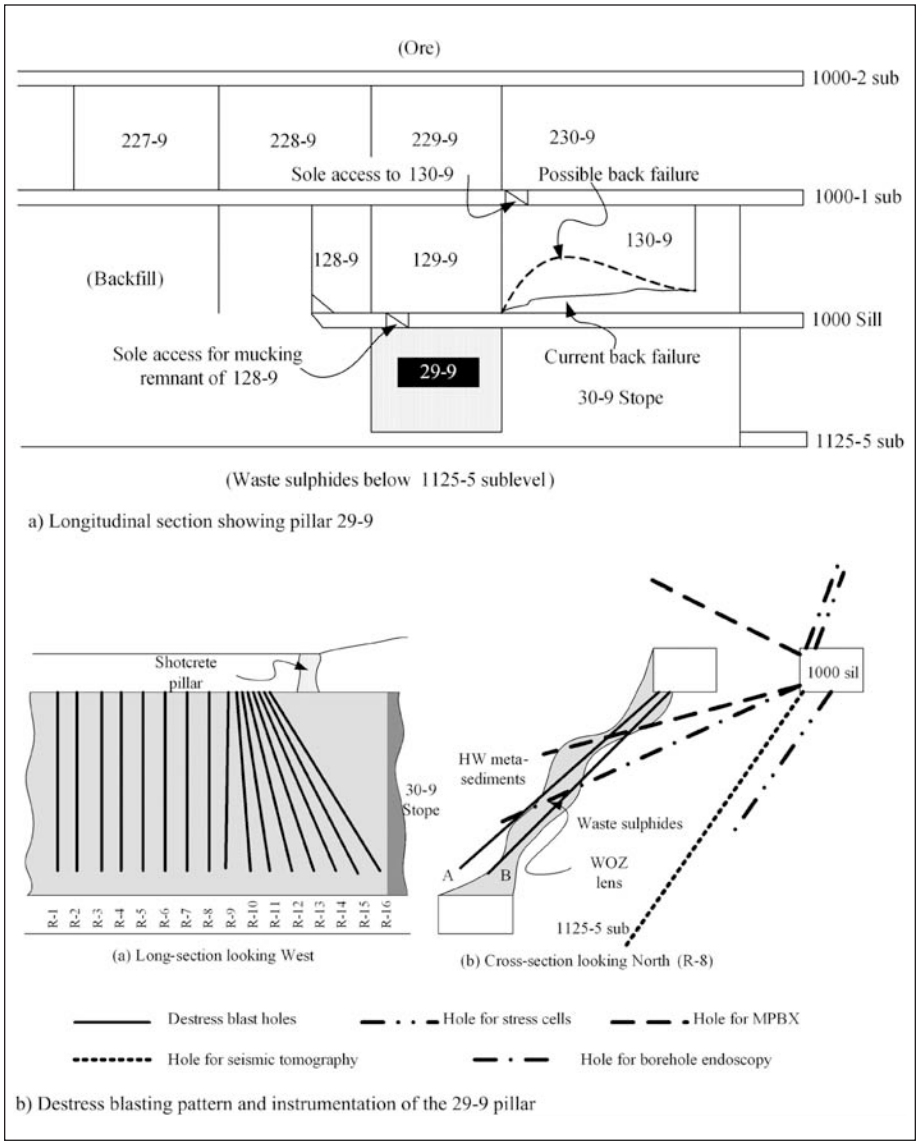

Fig. 8. Large-scale pillar destressing at Brunswick mine (adapted from Andrieux et al., 2003).

Discussion and Conclusion

The case studies presented in this paper bring about some interesting points regarding the effectiveness of destress blasting and how its effect is perceived differently by rock mechanics specialists.

The first case study of Strathcona mine reports damage in the drifts (supported with wire-mesh and rockbolts) due to the occurrence of a rockburst event of 2.7 Nuttli magnitude. The rockburst occurred concurrently with destress blasting. While the release of seismic energy with a destress blast is a desired feature, it is evident from the study that the notion of measuring success of destress blasting simply on the basis of the release of more seismic energy warrants further examination.

In the second case study of the Star Mine, attempts were made to destress the orebody itself before actual stoping operations took place. It was attempted with the hope that the benefits of destress blasting can be enjoyed over a longer period of time (up to the life of the stope). This line of thinking is diametrically opposite to the South African philosophy where the effect of destress blasting is only temporary; it lasts only for a few or so hours. Further, the case study highlights the need for careful mine planning before an application of destress blasting. It was reported that apart from the benefit of destress blasting, the exercise resulted in the transfer of stresses to other parts of the mine causing damages as well as ground control problems in the destressed stope.

The last case study of the Brunswick mine is the most recent attempt of large-scale pre-conditioning. The study involved 165 mm diameter blastholes charged with a powder factor of 2.5 kg/m^3, and yet the results showed no evidence of meaningful fracturing,

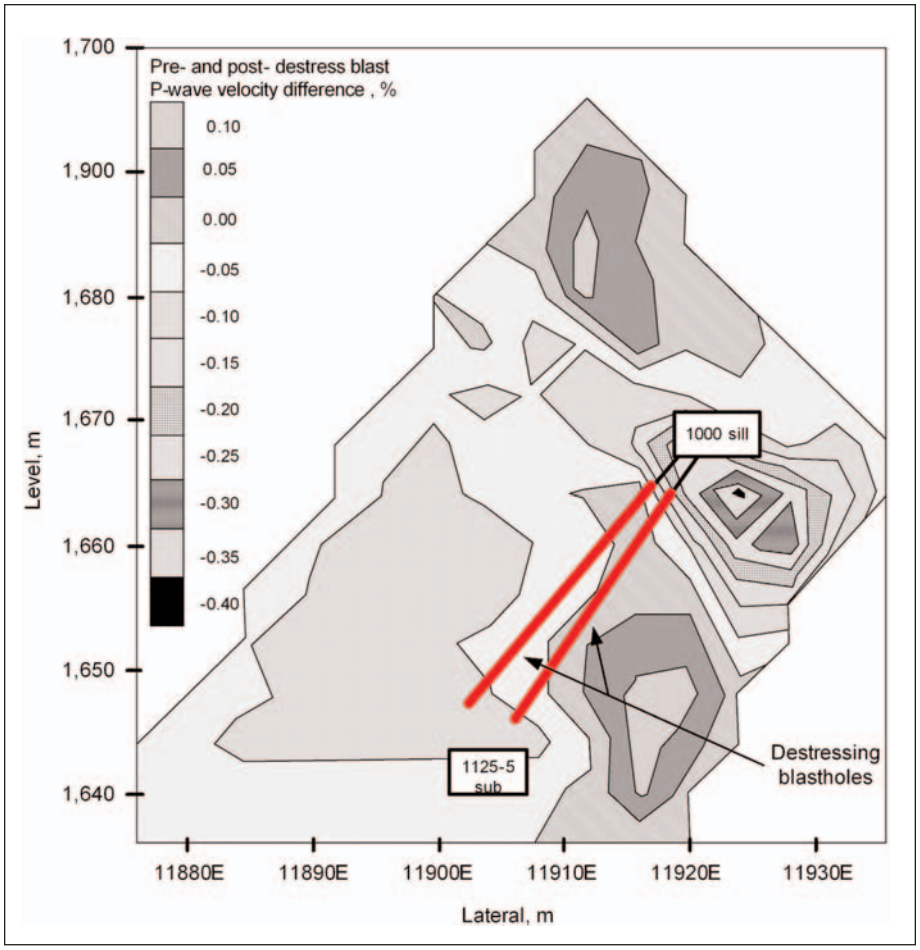

Fig. 9. Damage zone identification with pre- and post-destress blast seismic tomography at the Brunswick mine (longitudinal-section; Andrieux et al., 2003).

as indicated from cross-hole seismic tomography, borehole endoscopy, and a change in P-wave velocity before and after the destress balst. This could question the ability of destress blasting in creating new and/or meaningful fractures.

In summary, these case studies underline the fact that destress blasting is still poorly understood in spite of numerous research efforts and generous support from the mines and government agencies over a long period of time. There is a need to undertake the research at a micro-mechanical level to understand the development and growth of blast-generated fractures in confined rock mass and associated changes in the stress regime due to this dynamic fracture growth. An investigation of this nature is currently underway at McGill University.

Acknowledgment

The work presented in the paper is part of the research work done for the Ph.D. thesis of the second author. The research work was financially supported partially by the Natural Sciences and Engineering Research Council of Canada (NSERC) and the J.W. McConnel Foundation, McGill University. The authors are grateful for their support.

References

ADAMS, G.R., JAGER, A., and ROERING, G., 1981. Investigations of rock fractures around deep-level gold mine stopes. Proceedings, 22nd U.S. Rock Mechanics Symposium. Massachusetts Institute of Technology, p. 213-218.

ADAMS, D.J., GAY, N.C., and CROSS, M., 1993. Preconditioning: A technique for controlling rockbursts. *In* Proceedings, Rockbursts and Seismicity in Mines. *Edited by* R.P. Young. Queen's University, Balkema, Rotterdam, p. 29-33.

ANDRIEUX, P.P., BRUMMER, R.K., LIU, Q., SIMSER, B.P., and MORTAZAVI, A., 2003. Large-scale panel destress blast at Brunswick mine. CIM Bulletin, 1075, p. 78-87.

ANONYMOUS, 1939. Underground bumps at Crows Nest Pass. Iron and Coal Trade Reviews, 139, p. 341.

BLAKE, W., 1972a. Rockburst mechanics. Quarterly of the Colorado School of Mines, 67, p. 1-64.

BLAKE, W., 1972b. Destressing test at the Galena mine, Wallace, Idaho. Transactions, SME-AIME, 252, p. 294-299.

BLAKE, W., 1982. Rock preconditioning as a seismic control measure in mines. Proceedings, 1st International Congress on Rockbursts and Seismicity in Mines. South African Institute of Mining and Metallurgy, p. 225-229.

BLAKE, W., 1998. Destressing to control rock bursting. Underground Mining Methods Handbook, Chapter 7. Society for Mining, Metallurgy and Exploration, Colorado, p. 1535-1539.

BOARD, M.P. and FAIRHURST, C., 1983. Rockburst control through destressing, a case example. Proceedings, Symposium on Rockbursts: Prediction and Control. Institute of Materials, Metals and Mining, p. 91-102.

BRAUNER, G., 1994. Rockbursts in Coal Mines and their Prevention. Balkema, Rotterdam. 114 p.

BROWN, E.T., 1984. Rockbursts: prediction and control. Tunnels and Tunnelling, April, p. 17-19.

BRUMMER, R.K. and ANDRIEUX, P.P., 2002. A design methodology for destress blasting. *In* Proceedings, 5th North American Rock Mecanics Symposium (NARMS-TAC 2002)—Mining and Tunnelling Innovation and Opportunity. *Edited by* R. Hammah, W. Bawden, J. Curran, and M. Telesnicki. University of Toronto, p. 165-172.

BRUMMER, R.K. and RORKE, A.J., 1988. Case studies on large rockbursts in South African gold mines. *In* Proceedings, 29th US. Symposium on Rock Mechanics—Key questions in rock mechanics. *Edited by* P.A. Cundall, R.L. Sterling, and A.M. Starfield, p. 323-329.

CHRISTIAN, I.D., 1939. Rockbursts at the Teck-Hughes Mines. CIM Bulletin. 331, p. 530-567.

COOK, J.F. and BRUCE, D., 1983. Rockbursts at Macassa mine and the Kirkland Lake mining area. Proceedings, Symposium on Rockbursts: Prediction and Control. Institute of Materials, Metals and Mining, p. 81-90.

CORP, E.L., 1981. Rock mechanics research in the Coeur d'Alene mining district. Proceedings, Conference on the Application of Rock Mechanics to Cut and Fill Mining. Institution of Mining and Metallurgy, London, p. 40-48.

CRRP, 1996. A comprehensive summary of five years of collaborative research on rockbursting in hard rock mines. CAMIRO Mining Division, Canadian Rockburst Research Program, Book 1, Volume 2, Chapter 2, 37 p.

DICKHOUT, M.H., 1962. Ground control at the Creighton mine of the International Nickel Company of Canada Limited. Proceedings, 1st Canadian Rock Mechanics Symposium. McGill University, p. 121-139.

GAY, N.G., SPENCER, D., VAN WYK, J.J., and VAN DER HEEVER, P.K., 1984. The control of geological and mining parameters on seismicity in the Klerksdrop gold mine district. *In* Proceedings, 1st International Congress on Rockbursts and Seismicity in Mines. *Edited by* N.C. Gay and E.H. Wainwright. South African National Group on Rock Mechanics. The South African Institute of Mining and Metallurgy, p. 107-120.

HANSON, D., QUESNEL, W., and HONG, R., 1987. Destressing a Rockburst Prone Crown Pillar Macassa Mine. Division Report MRL 8782(TR), CANMET, Energy, Mines and Resources.

HANSON, D., MALINSKI, D., KAZAKIDIS, V., LAVERDURE, L., and BRUMMER, R.K., 1992. The design and evaluation of a destress blast at Strathcona mine. Proceedings, 16th Canadian Rock Mechanics Symposium. Laurentian University, p. 35-42.

HEDLEY, D.G.F., 1992. Rockburst Handbook for Ontario Hardrock Mines. CANMET Special Report SP921 E, ISBN-660-14549-9, 305 p.

HILL, F.G. and PLEWMAN, R.P., 1957. Destressing: A means of ameliorating rockburst conditions, Part 2—Implementing destressing with a discussion of the results so far obtained. Journal of the South African Institute of Mining and Metallurgy, 58, p. 269-277.

KAISER, P.K., 1993. Support of tunnels in burst-prone ground—Towards a rational design methodology. *In* Proceedings, 3rd International Symposium on Rockbursts and Seismicity in Mines. *Edited by* R.P. Young. Queen's University, p. 13-27.

KARWOSKI, W.J., MCLAUGHIN, W.C., and BLACK, W., 1979. Rock Preconditioning to Prevent Rock Bursts Report on a Field Demonstration. United States Department of the Interior, Bureau of Mines, Report of investigations 8381, 47 p.

LABRIE, D., PLOUFFE, M., HARVEY, A., and MAJOR, C., 1997. Destress blast testing at Sigma Mine: experimentation and results. Proceedings, 19th Session on Blasting Techniques of the Societé d'Energie Explosive du Québec, 26 p.

LIGHTFOOT, N., GOLDBACH, O.D., KULLMANN, D.H., and TOPER, A.Z., 1996. Rockburst control in the South African deep level gold mining industry. *In* Proceedings, 2nd North American Rock Mechanics Symposium, NARMS '96. *Edited by* M. Aubertin, F. Hassani, and H. Mitri. McGill University, p. 295-303.

LIU, Q., BLAINE, E., and CHUNG, S., 2003. Advanced blasting technology for large scale destress blast at Brunswick mine. Proceedings, CIM Mining Conference and Exhibition. The Canadian Institute of Mining, Metallurgy and Petroleum.Website: www.cim.org.

MACDONALD, P., WILES, T., and VILLENEUVE, T., 1988. Rock Mechanics aspects of vertical retreat mining at 2000 m depth at Creighton mine. Proceedings, CARE 88. Institute of Materials, Minerals and Mining, p. 151-158.

MCINNES, D., WILTON-CLARK, H., and MCLACHLAN, T., 1959. Report of the Royal Commission on the bump in Springhill No. 2 mine, October 23, 1958. Queen's Printer, Ottawa.

MITRI, H.S., SCOBLE, M.J., and MCNAMARA, K., 1988. Numerical studies of destressing mine pillars in highly stressed rock. Proceedings, 41st Canadian Geotechnical Conference. Canadian Geotechnical Society, p. 50-56.

MITRI, H.S., 1996. Study of rockburst potential at Sigma mine, Val D'Or, Quebec, using numerical modelling. Final Report, 125 p.

MITRI, H.S., 2000. Practitioner's guide to destress blasting in hard rock mines. Department of Mining, Metals and Materials Engineering, McGill University, 181 p.

MITRI, H.S., TANG, B., and SIMON, R., 1999. FE modeling of mining-induced energy release and storage rates. Transactions, Journal of the South African Institute of Mining and Metallurgy 99, p. 103-110.

MORRISON, R.G.K., 1942. Report on rockburst situation in Ontario mines. Transactions, Canadian Institute of Mining and Metallurgy, 45, p. 225-272.

MORUZI, G.A. and PASIEKA, A.R., 1969. Evaluation of a blasting technique for destressing ground subject to rockburting. Proceedings, 5th Canadian Symposium on Rock Mechanics, p. 185-204.

O'DONNELL, J.D.P., 1992. The use of destress blasting at Inco's Creighton mine. Proceedings, MASSMIN '92. The South African Institute of Mining and Metallurgy, p. 71-74.

OLIVER, P., WILES, T., MACDONALD, P., and O'DONNELL, D., 1987. Rockburst control measures at Inco's Creighton mine. Proceedings, 6th Conference on Ground Control in Mining. University of West Virginia.

RORKE, A.J., CROSS, M., VAN ANTWERPEN, H.E.F., and NOBLE, E., 1990. The mining of a small updip remnant with the aid of preconditioning blasts. Proceedings, International Deep Mining Conference, Series S10. The South African Institute of Mining and Metallurgy Symposium, p. 765-774.

ROUX, A.J.A., LEEMAN, E.R., and DENKHAUS, H.G., 1957. Destressing: A means of ameliorating rockburst conditions, Part 1—The concept of destressing and results obtained from its application. The South Africa Institute of Mining and Metallurgy, p. 101-127.

SALAMON, M.D.G., 1970. Stability, instability and design of pillar workings. International Journal of Rock Mechanics and Mining Sciences, 7, p. 613-631.

SALAMON, M.D.G., 1974. Rock mechanics of underground excavations. Advances in Rock Mechanics, Volume 1-B. Proceedings, 3rd Congress. International Society of Rock Mechanics, p. 951-1099.

SCOBLE, M.J., CULLEN, M., and MAKUCH, A., 1987. Experimental studies of factors relating to destress blasting. *In* Proceedings, 28th U.S. Symposium on Rock Mechanics. *Edited by* H.L. Hartman. University of Arizona, p. 901-908.

STAROSELTSEV, V.S. and SYSOLYATIN, F.V., 1979. Experience of combating rockbursts at the Kizel coal basin mines. Proceedings, VI All-Union Conference on Rock Mechanics—Rockbursts, Methods of Estimation and Control of Rockmass Rockburst Hazards. The Kirg Soviet Socialist Republic Science Academy, Institute of Physics and Mechanics of Rocks, p. 236-242 (in Russian).

TANG, B., 2000. Rockburst Control Using Destress Blasting. Ph.D. thesis, McGill University, Montreal, 178 p.

TANG, B. and MITRI, H., 2001. Numerical modelling of rock preconditioning by destress blasting. Ground Improvement, 5, p. 57-67.

TOPER, A.Z, GRODNER, M., STEWART, R.D., and LIGHTFOOT, N., 1997. Preconditioning: A rockburst control technique. *In* Proceedings, 4th International Symposium on Rockbursts and Seismicity in Mines. *Edited by* S.J. Gibowicz and S. Lasocki. Balkema, Rotterdam, p. 267-272.

WIGGILL, R.B., 1963. The effects of different support methods on strata behaviour around stoping excavations. Journal of the South African Institute of Mining and Metallurgy, 63, p. 391-425.

WILLAN, J., SCOBLE, M., and PAKALNIS, V., 1985. Destressing practice in rockburst prone ground. Proceedings, 4th Conference on Ground Control in Mining. West Virginia University, p. 135-147.

WILLIAMS, T.J. and CUVELLIER, D.J., 1988. Report on a field trial of an underhand longwall mining method to alleviate rockburst hazards. Proceedings, 2nd International Symposium on Rockbursts and Seismicity in Mines. University of Minnesota, p. 349-354.